MIAMI UNIVERSITY

The Graduate School

Certificate for Approving the Dissertation

We hereby approve the Dissertation

of

Zachary Callahan

Candidate for the Degree:

DOCTOR OF PHILOSOPHY

_____

Director
Paul Schaeffer

_____

Reader
Paul Harding

_____

Reader
Paul James

_____

Reader
Haifei Shi

_____

Graduate School Representative
Doug Noe

ABSTRACT

THE INDEPENDENT EFFECTS OF CHRONIC HIGH-FAT FEEDING AND LONG-TERM DENERVATION IN RELATION TO DEVELOPMENT OF DIABETES

by Zachary J. Callahan

Type 2 diabetes is a characterized by a variety of metabolic perturbations including reduced insulin sensitivity, increased plasma glucose levels, and metabolic inflexibility. However, there is a lack of information investigating the temporal transition from a healthy to a disease state. This dissertation describes two studies that examined the independent effects of obesity and inactivity on the pathophysiology of diabetes.

The first study focused on inactivity, using denervation of the sciatic nerve to identify and describe the effects that prolonged inactivity has on glucose transport, insulin signaling, and expression of genes involved in regulation of mitochondrial transcription. Although GLUT4 mRNA expression was significantly lower in muscle from denervated mice at all time points, GLUT4 protein was lower only during the first 3 weeks. GLUT 4 protein expression was higher in both the 28 and 56 days post-surgery animals. Protein expression of Akt, was also elevated in tissue from denervated muscle. Genes involved in transcriptional regulators of metabolism, glycolysis, and fatty-acid transport were all significantly lower in denervated tissue. These results suggest that short-term results noted in previous denervation studies may not be representative of long-term effects of inactivity and that there may be compensatory mechanisms that improve glucose uptake.

The second study investigated the effects that prolonged high-fat feeding would have on body composition, mitochondrial function, intramuscular triglyceride (IMTG) content, and glucose metabolism. Using a transgenic mouse model that is susceptible to the development of a diabetic phenotype, we demonstrated that high-fat fed mice had significantly greater body mass and IMTG than normal-chow fed mice. Results from a glucose tolerance test revealed a larger glucose area-under-the-curve in transgenic mice fed a high-fat diet, indicating that these animals were beginning to develop a diabetic phenotype. There was no significant difference in cytochrome C oxidase enzyme activity at any time point among any groups and citrate synthase activity was greater only in the 24-week high-fat fed transgenic mice. Finally, there was no difference in genes encoding transcriptional regulators of metabolism or fatty acid metabolism. These results suggest that high-fat feeding leads to obesity and changes in body composition with increases in IMTG content and decrements in glucose metabolism before evidence of mitochondrial dysfunction.

THE INDEPENDENT EFFECTS OF CHRONIC HIGH-FAT FEEDING AND LONG-TERM DENERVATION IN RELATION TO DEVELOPMENT OF DIABETES

A Dissertation

Submitted to the Faculty of
Miami University in partial
fulfillment of the requirement
for the degree of
Doctor of Philosophy
Department of Biology

by

Zachary J. Callahan
Miami University
Oxford, Ohio
2014

Dissertation Director: Paul J. Schaeffer

TABLE OF CONTENTS

Item	Page
Table of contents	**iii**
List of tables	**v**
List of figures	**vi**
Acknowledgements	**ix**
Chapter 1: General Introduction	**1**
References	**4**
Chapter 2: Compensatory responses of the insulin-signaling pathway restore muscle glucose uptake following long-term denervation	**7**
Abstract	**8**
Introduction	**9**
Materials and Methods	**10**
Results	**14**
Discussion	**16**
References	**21**
Tables	**25**
Figure Legends	**26**
Figures	**28**
Chapter 3: Prolonged high-fat feeding increases intramuscular triglycerides content and decreases glucose metabolism, but does not affect mitochondrial function	**48**
Abstract	**49**
Introduction	**50**
Materials and Methods	**53**
Results	**57**

Discussion **60**
References **63**
Tables **69**
Figure Legends **70**
Figures **72**

Chapter 4: Concluding remarks **81**

LIST OF TABLES

Item		Page
Chapter 2:		
Table 2.1	Primer sequences for qPCR	**24**
Chapter 3:		
Table 3.1	Primer sequences for qPCR	**68**

LIST OF FIGURES

Item **Page**

Chapter 2:

Figure 2.1 **27**

Denervation leads to rapid initial weight loss in hind-limb muscles with no subsequent loss after 28 days post surgery.

Figure 2.2 **30**

Myocellular cross-sectional area is reduced following denervation surgery.

Figure 2.3 **33**

mRNA expression is lower for genes involved in metabolic regulation in denervated GC muscle throughout time course of study.

Figure 2.4 **37**

mRNA expression is lower for genes regulating metabolic enzymes in denervated GC muscle throughout time course of study.

Figure 2.5 **42**

Skeletal muscle glucose uptake and transport improves in response to chronic denervation over the course of long-term denervation.

Figure 2.6 **43**

A. GLUT4 protein expression is higher in chronically denervated GC muscle while GLUT4 gene expression is lower

in chronically denervated GC muscle. B. GLUT1 protein expression is higher in chronically denervated GC muscle. GLUT1 gene expression is not different in chronically denervated GC muscle.

Figure 2.7 **45**

The response of Akt2 to chronic denervation suggests compensation to maintain insulin signaling in GC muscle.

Chapter 3:

Figure 3.1 **71**

High-fat chow leads to increases in body mass in transgenic mice.

Figure 3.2 **73**

Transgenic mice fed high-fat chow have higher intramuscular lipid content.

Figure 3.3 **74**

Plasma insulin concentration is higher in transgenic mice fed high-fat chow.

Figure 3.4 **75**

Glucose area under the curve is higher in TGHF mice.

Figure 3.5 **76**

Citrate synthase activity is higher at 24 weeks in TGHF fed mice compared to TGCH mice, but cytochrome c oxidase activity is unchanged at any time point in homogenates of gastrocnemius muscle.

Figure 3.6 **78**

mRNA expression is not statistically different for genes involved in metabolic regulation in all groups throughout the time course of the study.

Figure 3.7 **79**

mRNA expression is not statistically different for genes involved in fatty acid transport and mitochondrial function in all groups throughout the time course of the study.

ACKNOWLEDGEMENTS

I would like to thank Paul Schaeffer for his support and guidance in the completion of this project as well as his contributions to my professional and academic development. Thanks also to the members of my dissertation committee, Paul Harding, Paul James, Douglas Noe, and Haifei Shi whose advice was invaluable in improving this work. Additional thanks to Michael Hughes and the Miami University Statistical Consulting Center, who provided statistical assistance. It was a privilege to collaborate with other members of the Schaeffer lab, particularly, Amanda Bartos, Emily Cassell, Keely Corder, Kristen DeMoranville, Chelsea Menke, Patrick Mineo, and Michael Oxendine. This work would also not have been possible without the assistance of the Geiger lab, including Paige Geiger and Josh Wheatley. Finally, I would like to thank my friends and family, most especially my wife Tricia, my daughters Kathryn and Olivia, and my mother Marte for supporting and encouraging me through my academic career.

CHAPTER 1
GENERAL INTRODUCTION

Type 2 diabetes is a chronic, multifactorial disease, characterized by a variety of metabolic perturbations including reduced insulin sensitivity, increased plasma glucose levels, and metabolic inflexibility. Often described as a lifestyle disease, some common risk factors for developing diabetes include obesity, inactivity, hypertension, and dyslipidemia. One of the major challenges associated with the diagnosis or prevention of diabetes is that it may take 10-20 years, or longer, for symptoms to surface. Approximately 10% of the adult US population is diabetic and this percentage is projected to increase anywhere from 33-50% by the year 2050 (3). The exponential increase in the incidence of diabetes is not limited to the United States, with approximately ~382 million diabetics worldwide and an expected rise to 592 million by 2035 (7). Diabetes is the 6th leading cause of death in the United States and 7th worldwide, a statistic made even more imposing when considering that ¼ of those in the US and ½ worldwide with diabetes are unaware that they have the disease (3, 18). The economic costs associated with diabetes are staggering as well, with an estimated economic cost of $245 billion in 2012, just in the United States (3). These factors place a huge burden on our healthcare system and clearly demonstrate a need for further research into the mechanisms involved in the development and prevention of diabetes.

Two of the primary risk factors associated with diabetes are excess adiposity and inactivity. Approximately 80% of those diagnosed with type 2 diabetes are also overweight or obese (1). Increases in both visceral adiposity and intramuscular triglycerides (IMTG) are seen in obese, diabetic populations. There is also a strong correlation between increased IMTG content and insulin resistance (15, 26, 27). Mitochondrial dysfunction and an inability for metabolic flexibility, the capacity to transition effectively between lipid and carbohydrate metabolism, are also strongly associated with diabetes (6, 13, 20, 22). However, what is unclear is whether increases in IMTG drive perturbations in mitochondrial dysfunction and the development of diabetes or if mitochondrial dysfunction drives the accumulation of IMTG, leading to decrements in insulin sensitivity and the development of diabetes.

The report that an increase in intracellular lipids in pancreatic tissue led to increases in β-cell death was cause for proposition of a "lipotoxicity" theory that ectopic lipid accumulation drives mitochondrial dysfunction and the subsequent development of metabolic disorders (32). However, subsequent research noted that endurance athletes also have high levels of intramuscular triglycerides, yet do not demonstrate any impairment in insulin sensitivity or metabolic flexibility (8, 10, 25). Long-term studies examining the temporal relationship between mitochondrial function and IMTG content under conditions of increasing obesity and a diabetic phenotype are lacking.

The paradox of elevated IMTG content without decrements in metabolic flexibility and insulin sensitivity seen in athletes implies that activity can offer some protection against diabetes. Exercise has been shown to improve metabolic flexibility and increase mitochondrial function as well as improve insulin sensitivity (9, 12, 24). Additionally, studies have shown that exercise decreases risk factors associated with metabolic syndrome through improvements in plasma glucose levels and cardiorespiratory function as well as decreased adiposity (23, 30). Although the beneficial effects of exercise are clear, the mechanisms responsible for the negative effects that inactivity has on health are less understood. It has been proposed that inactivity increases the risk of cardiovascular disease, drives the development of many other metabolic disorders, including diabetes, and accelerate the aging process (4, 17, 21). Skeletal muscle is profoundly affected by inactivity with noted atrophy-related reductions in power and tissue mass (14, 16, 29). As skeletal muscle accounts for a majority of glucose homeostasis, decrements in muscle mass have a profound effect on glucose uptake and whole-body glucose metabolism. Denervation is commonly used to simulate the effects of inactivity and isolate inactivity from obesity. Most studies investigating the effect that denervation has on glucose metabolism have focused on short-term effects up to 17 days post-surgery (2, 5, 11, 19, 31). In the first few weeks after denervation, there are profound changes to muscle, including large decreases in mass and glucose uptake (2, 5, 11, 19, 28, 31). However, the rapid rate of atrophy slows significantly by 25-30 days post-surgery, with almost no further loss of muscle mass reported after this time point (28). There has been limited research on long-term denervation and it is possible that the severe up-regulation of atrophic pathways seen

during this time interval is not an accurate representation of future metabolic parameters, such as glucose uptake, insulin-signaling, and mitochondrial regulation.

Therefore, this dissertation sought to investigate the independent, temporal effects that obesity (via prolonged high-fat feeding) and inactivity (via long-term denervation) have on glucose metabolism and mitochondrial function. The focus of the first project was inactivity, using long-term denervation as a model to isolate inactivity effects from obesity effects. In this project, we investigated the temporal changes in mitochondrial regulation, glucose uptake, and components of the insulin-signaling pathway to see if there were compensatory responses after the initial upregulation of atrophic pathways. The second project focused on obesity related changes by investigating the temporal changes that high-fat feeding had on body composition, glucose metabolism, IMTG content, and mitochondrial function contrasted against normal chow fed mice. Together, these two projects will further knowledge about the temporal changes associated with obesity and inactivity during the development of a diabetic condition.

REFERENCES

1. Astrup A, Finer N. Redefining type 2 diabetes: “diabesity” or “obesity dependent diabetes mellitus”? *Obes Rev* 1: 57–59, 2000.

2. Block NE, Menick DR, Robinson KA, Buse MG. Effect of denervation on the expression of two glucose transporter isoforms in rat hindlimb muscle. *J Clin Invest* 88: 1546–52, 1991.

3. Boyle JP, Thompson TJ, Gregg EW, Barker LE, Williamson DF. Projection of the year 2050 burden of diabetes in the US adult population: dynamic modeling of incidence, mortality, and prediabetes prevalence. *Popul Health Metr* 8: 29, 2010.

4. Cherkas LF, Hunkin JL, Kato BS, Richards JB, Gardner JP, Surdulescu GL, Kimura M, Lu X, Spector TD, Aviv A. The association between physical activity in leisure time and leukocyte telomere length. *Arch Intern Med* 168: 154–8, 2008.

5. Coderre L, Monfar MM, Chen KS, Heydrick SJ, Kurowski TG, Ruderman NB, Pilch PF. Alteration in the expression of GLUT-1 and GLUT-4 protein and messenger RNA levels in denervated rat muscles. *Endocrinology* 128: 1821–1825, 1991.

6. Corpeleijn E, Saris WHM, Blaak EE. Metabolic flexibility in the development of insulin resistance and type 2 diabetes: effects of lifestyle. *Obes Rev* 10: 178–93, 2009.

7. Danaei G, Finucane MM, Lu Y, Singh GM, Cowan MJ, Paciorek CJ, Lin JK, Farzadfar F, Khang Y-H, Stevens G a, Rao M, Ali MK, Riley LM, Robinson C a, Ezzati M. National, regional, and global trends in fasting plasma glucose and diabetes prevalence since 1980: systematic analysis of health examination surveys and epidemiological studies with 370 country-years and 2·7 million participants. *Lancet* 378: 31–40, 2011.

8. Dubé JJ, Amati F, Stefanovic-Racic M, Toledo FGS, Sauers SE, Goodpaster BH. Exercise-induced alterations in intramyocellular lipids and insulin resistance: the athlete’s paradox revisited. *Am J Physiol Endocrinol Metab* 294: E882–E888, 2008.

9. Friedlander AL, Jacobs KA, Fattor JA, Horning MA, Hagobian TA, Bauer TA, Wolfel EE, Brooks GA. Contributions of working muscle to whole body lipid metabolism are altered by exercise intensity and training. *Am J Physiol Endocrinol Metab* 292: E107–16, 2007.

10. Goodpaster BH, He J, Watkins S, Kelley DE. Skeletal muscle lipid content and insulin resistance: Evidence for a paradox in endurance-trained athletes. *J Clin Endocrinol Metab* 86: 5755–5761, 2001.

11. Henriksen EJ, Rodnick KJ, Mondon CE, James DE, Holloszy JO. Effect of denervation or unweighting on GLUT-4 protein in rat soleus muscle. *J Appl Physiol* 70: 2322–2327, 1991.

12. Holloszy JO, Coyle EF. Adaptations of skeletal muscle to endurance exercise and their metabolic consequences. *J Appl Physiol* 56: 831–8, 1984.

13. Kelley DE, He J, Menshikova E V., Ritov VB. Dysfunction of Mitochondria in Human Skeletal Muscle in Type 2 Diabetes. *Diabetes* 51: 2944–2950, 2002.

14. Kim JH, Thompson LV. Inactivity, age, and exercise: single-muscle fiber power generation. *J Appl Physiol* 114: 90–8, 2013.

15. Krssak M, Falk Petersen K, Dresner A, DiPietro L, Vogel SM, Rothman DL, Roden M, Shulman GI. Intramyocellular lipid concentrations are correlated with insulin sensitivity in humans: a 1H NMR spectroscopy study. *Diabetologia* 42: 113–6, 1999.

16. Lawler JM, Hindle A. Living in a box or call of the wild? Revisiting lifetime inactivity and sarcopenia. *Antioxid Redox Signal* 15: 2529–41, 2011.

17. Lees SJ, Frank W. Sedentary Death Syndrome Introduction: Inactivity is an Actual Cause of Death. *Canadian Journal of Applied Physiology.* 29: 447–460, 2004.

18. Mathers CD, Loncar D. Projections of Global Mortality and Burden of Disease from 2002 to 2030. *PLoS Med* 3: e442, 2006.

19. Megeney LA, Neufer PD, Dohm GL, Tan MH, Blewett CA, Elder GC, Bonen A. Effects of muscle activity and fiber composition on glucose transport and GLUT-4. *Am J Physiol* 264: E583–E593, 1993.

20. Mootha VK, Lindgren CM, Eriksson K-F, Subramanian A, Sihag S, Lehar J, Puigserver P, Carlsson E, Ridderstråle M, Laurila E, Houstis N, Daly MJ, Patterson N, Mesirov JP, Golub TR, Tamayo P, Spiegelman B, Lander ES, Hirschhorn JN, Altshuler D, Groop LC. PGC-1alpha-responsive genes involved in oxidative phosphorylation are coordinately downregulated in human diabetes. *Nat Genet* 34: 267–273, 2003.

21. Morris JN, Heady JA, Raffle PAB, Roberts CG, Parks JW. Coronary Heart Disease and Physical Activity of Work. *Lancet* 262: 1053–1057, 1953.

22. Patti ME, Butte AJ, Crunkhorn S, Cusi K, Berria R, Kashyap S, Miyazaki Y, Kohane I, Costello M, Saccone R, Landaker EJ, Goldfine AB, Mun E, DeFronzo R, Finlayson J, Kahn CR, Mandarino LJ. Coordinated reduction of genes of oxidative metabolism in humans with insulin resistance and diabetes: Potential role of PGC1 and NRF1. *Proc Natl Acad Sci U S A* 100: 8466–8471, 2003.

23. Pattyn N, Cornelissen VA, Eshghi SRT, Vanhees L. The effect of exercise on the cardiovascular risk factors constituting the metabolic syndrome: a meta-analysis of controlled trials. *Sports Med* 43: 121–33, 2013.

24. Phielix E, Meex R, Moonen-Kornips E, Hesselink MKC, Schrauwen P. Exercise training increases mitochondrial content and ex vivo mitochondrial function similarly in patients with type 2 diabetes and in control individuals. *Diabetologia* 53: 1714–21, 2010.

25. Russell AP. Lipotoxicity: the obese and endurance-trained paradox. *Int J Obes Relat Metab Disord* 28 Suppl 4: S66–S71, 2004.

26. Savage DB, Petersen KF, Shulman GI. Disordered lipid metabolism and the pathogenesis of insulin resistance. *Physiol Rev* 87: 507–20, 2007.

27. Schaffer JE. Lipotoxicity: when tissues overeat. *Curr Opin Lipidol* 14: 281–287, 2003.

28. Thomason DB, Booth FW. Atrophy of the soleus muscle by hindlimb unweighting. *J Appl Physiol* 68193: 1–12, 1990.

29. Thompson LV. Skeletal muscle adaptations with age, inactivity, and therapeutic exercise. *J Orthop Sports Phys Ther* 32: 44–57, 2002.

30. Touati S, Meziri F, Devaux S, Berthelot A, Touyz RM, Laurant P. Exercise reverses metabolic syndrome in high-fat diet-induced obese rats. *Med Sci Sports Exerc* 43: 398–407, 2011.

31. Turinsky J. Dynamics of insulin resistance in denervated slow and fast muscles in vivo. *Am J Physiol* 252: R531–R537, 1987.

32. Unger RH. Lipotoxicity in the pathogenesis of obesity-dependent NIDDM: Genetic and clinical implications. *Diabetes* 44: 863–870, 1995.

CHAPTER 2

Compensatory responses of the insulin-signaling pathway restore muscle glucose uptake following long-term denervation

ABSTRACT

We investigated the role of muscle activity in maintaining normal glucose homeostasis via transection of the sciatic nerve, an extreme model of disuse atrophy. Mice were sacrificed 3, 10, 28, or 56 days after transection or sham surgery. There was no difference in muscle weight between sham and transected limbs at 3 days post-surgery, but it was significantly lower following transection at the other three time points. Transected muscle weight stabilized by 28 days post-surgery with no further loss. Myocellular cross sectional area was significantly smaller at 10, 28 and 56 days post-transection surgery. Additionally, muscle fibrosis area was significantly greater at 56 days post-transection. In transected muscle there was reduced expression of genes encoding transcriptional regulators of metabolism (PPARα, PGC-1α, PGC-1β, PPARδ), a glycolytic enzyme (PFK), a fatty acid transporter (M-CPT 1), and an enzyme of mitochondrial oxidation (CS) with transection. In denervated muscle, glucose uptake was significantly lower at 3 days but was greater at 56 days under basal and insulin-stimulated conditions. Although GLUT 4 mRNA was significantly lower at all time points in transected muscle, Western blot analysis showed greater expression of GLUT4 at 28 and 56 days post-surgery. GLUT1 mRNA was unchanged; however GLUT1 protein expression was also greater in transected muscles. Surgery led to significantly higher protein expression for Akt2 as well as higher phosphorylation of Akt. While denervation may initially lead to reduced glucose sensitivity, compensatory responses of insulin signaling appeared to restore and improve glucose uptake in long term transected muscle.

Keywords: Disuse atrophy, nerve transection, diabetes, Akt

INTRODUCTION

Incidence of type 2 diabetes is rising worldwide and the number of affected individuals is growing much faster than anticipated. In 1997 it was estimated that by 2020 the number of type 2 diabetics would be approximately 250 million people worldwide (27). However, two recent studies show that figure has already been eclipsed with an estimated number of adults with diabetes ranging from 287 million in 2009 (30) to 347 million in 2011 (9). Calculations using the lower value yielded a prediction of 439 million affected individuals by 2030 (30), with huge increases (up to 98% in some countries) seen throughout the world.

Clearly, many factors play a role in the pathogenesis of diabetes, but one of the primary components is activity. The benefits of increased activity in preventing metabolic diseases, including type 2 diabetes, have been discussed previously and include large reductions (58%) in the risk of impaired glucose tolerance progressing to type 2 diabetes, decreases in mortality, as well as improvements in blood pressure and blood lipids (32). Even brief light-to-moderate activity has a beneficial impact on the expression of genes involved in metabolism, as well as improving glucose metabolism (21). However, the effects of disuse atrophy on the regulation of normal metabolic function are less understood. As obesity is often associated with disuse atrophy, research isolating the effects of disuse atrophy on glucose uptake is ongoing. Attempts to mimic the effects of disuse atrophy have included suspension of the animal by the tail or immobilizing one hindlimb via denervation or stapling. Denervation has frequently been used to disrupt activity on a local scale and has been shown to impair glucose uptake as soon as 24 hours after surgery (4, 13, 25, 37). However, denervation of skeletal muscle initiates a cascade of events including rapid up-regulation of factors involved in apoptotic and necrotic pathways which further compromise normal cellular function, potentially including glucose uptake, as well as causing significant decreases in muscle mass (13, 25, 37). As previous studies have focused on short-term effects of denervation, it is unclear whether impaired glucose uptake is due to disuse atrophy, active apoptosis and necrosis, or a combination of these effects. It is well established that severe reductions in skeletal muscle mass due to denervation are temporally limited to the first 25-30 days, after which time the reduced mass is maintained indefinitely (34). By extending our investigation

beyond the time frame when apoptosis and necrosis are highly active, we will better elucidate the ability of skeletal muscle to import glucose during prolonged disuse atrophy.

Plasma glucose is imported intra-cellularly via the family of glucose transporters, including GLUT 1 and GLUT 4 (40). GLUT1 is distributed throughout the plasma membrane and functions in basal glucose uptake. GLUT4 however, is the primary transport mechanism for insulin-stimulated glucose uptake in both skeletal muscle and adipose tissue (31). An increase in insulin binding to its receptor initiates a signaling cascade that ultimately results in the translocation of GLUT4 from vesicles inside the cell to the cell membrane allowing facilitated diffusion of glucose into the cell (18, 28). It has been shown that exercise improves the capacity of skeletal muscle to import glucose into the cell (14). It has been proposed that disuse atrophy alone could promote pathogenesis of diabetes and other metabolic diseases (23), but the effects disuse atrophy has on glucose uptake or GLUT expression are less understood.

Here we examine for the first time the effect of long-term denervation on glucose uptake in skeletal muscle. In addition, we investigate expression of genes involved in mitochondrial oxidation, substrate transport, and regulation of metabolism. For these separate processes occurring in parallel, we have two hypotheses: 1) as demonstrated previously, transection surgery will lower glucose uptake in the days immediately following surgery, but glucose uptake will be improved in the later time points, and 2) transection surgery will initially lower expression of genes involved in regulation of metabolism, as well as substrate uptake and oxidation. We expect expression of these genes to improve with time as well.

MATERIALS AND METHODS

Animals and surgery

All animal experiments and euthanasia protocols were conducted in accordance with the National Institutes of Health guidelines for humane treatment of laboratory animals and were reviewed and approved by the Institutional Animal Care and Use Committee of Miami University.

C57BL/6J mice were obtained from Harlan Laboratories (Indianapolis, IN) and a

breeding colony was established at the Miami University Animal Care Facility (except those used for the functional glucose uptake). All mice were housed in cages under conditions of controlled temperature and humidity with a 12:12-h light:dark cycle and given standard chow and water ad libitum. Upon reaching 8 weeks of age, mice were anesthetized with isofluorane delivered via inhalation at 5% for induction, followed by reduction to 2% for maintenance. One hindlimb was denervated by surgical removal of a 1.0 cm segment of the sciatic nerve, which innervates the tibialis anterior (TA), extensor digitorum longus (EDL), gastrocnemius (GC), and soleus (SOL) muscles, as previously described (36). On the contralateral (sham) hindlimb, the sciatic nerve was visualized but not touched. After surgery, the mice were randomly assigned for sacrifice at 3, 10, 28, or 56 days post-surgery. Insulin (0.5U/mouse) or saline was injected (intraperitoneal) 10 minutes prior to sacrifice. Mice were euthanized by carbon dioxide inhalation, weighed and the hindlimb muscles were removed, weighed and frozen for subsequent analysis, except for the mice used for the glucose uptake assays (see below). In each of the experimental time points, muscles from the contralateral limb were used as an internal control.

C57BL/6J mice used in the glucose uptake assay were also obtained from Harlan Laboratories but were housed at the Kansas University Medical Center. Mice were housed and denervation surgery performed as above. After surgery, the mice were randomly assigned to glucose uptake experiments at 3, 10, 28, or 56 days post-surgery. Upon reaching terminal end points, pentobarbital was used to anesthetize the mice. Prior to euthanasia EDL muscles were removed, weighed and prepared as described below.

Histological analysis

TA muscles from control and denervated legs were frozen in liquid nitrogen-cooled 2-methyl butane and stored at -80°C. Cross-sections (12 μm) were cut using a cryostat (Micron HM 550, Thermo Scientific, Florence, KY) and sections were stained with Gomori trichrome following Engel and Cunningham (1963). ImageJ software (NIH) was used to measure total area of each section, area containing fibrotic tissue, and myocellular cross sectional area.

Protein analysis

Snap frozen GC samples were sonicated in RIPA buffer. Total protein concentration in muscle homogenates was determined via BCA assay. 50 µg of muscle protein extracts from GC were resolved by SDS-PAGE (7.5%) and subsequently transferred to nitrocellulose membranes. Membranes were blocked (1 hour at room temperature) with a 5% skim milk (5% BSA was used for p-Akt) in TBS-T [Tris-buffered saline and 0.1% Tween 20] solution. Blots were then incubated overnight at 4°C with anti-rabbit antibody directed against GLUT4 (ab654) or GLUT1 (ab652) (Abcam, Cambridge, MA), Akt2 (3063) or phospho-Akt Ser473 (9271) (Cell Signaling, Beverly, MA). After primary antibody incubation, blots were washed four times in TBS-T (1 × 15, 3 × 5 min.) and incubated with horseradish peroxidase (HRP)-linked goat anti-rabbit secondary antibody (Cell Signaling Technology; 1:1,000 dilution) at room temperature (60 min). Protein expression was assayed using enhanced chemiluminescence (Pierce-Thermo Fisher Scientific, Rockford, IL.) and quantified using Alphamager HP (Protein Simple, San Jose, CA). Values for 3-day sham were used to determine relative expression and Ponceau S staining was used to verify loading volumes.

Quantitative RT-PCR

Quantitative RT-PCR using 36B4 (acidic ribosomal phosphoprotein P0) as a control gene was used to assess expression levels of transcripts for various genes including: GLUT1 (Glucose transporter type 1), GLUT4 (Glucose transporter type 4), PPARα and PPARδ (Peroxisome proliferator-activated receptor alpha and beta/delta), PGC-1α and PGC-1β (PPAR gamma coactivator 1-alpha and beta), CD36 (Fatty Acid Translocase), MCAD (Medium-chain acyl-CoA dehydrogenase), PFK (Phosphofructokinase), M-CPT I (Muscle Carnitine Palmitoyltransferase I) and CS (Citrate Synthase). Primer efficiencies were verified for all genes investigated and all gene expression data were normalized to 36B4, which did not change with treatment.

Primers were obtained from Integrated DNA Technologies (Corralville, IA); see Table 2.1 for primer sequences. RNA was isolated from GC muscle using TRIzol (Life Technologies, Grand Island, NY) according to manufacturer's instructions. RNA quality was assessed spectrophotometrically (NanoDrop 1000, NanoDrop-Fisher Thermo

Scientific, Rockford, IL) and quantified by absorption spectrophotometry at 260 and 280 nm. cDNA was generated from the total RNA for each muscle using qScript™ cDNA Synthesis Kit (Quanta Biosciences, Gaithersburg, MD) according to the manufacturer's instructions. Relative quantitative RT-PCR was subsequently performed with a RotorGene 3000 (Qiagen, Valencia, CA) system using SYBR Green Master Mix (Applied Biosystems, Foster City, CA). For each gene, real-time PCR was performed in triplicate wells on cDNA generated from the reverse transcription of 10 ng of total RNA.

Functional Glucose Uptake

Freshly harvested EDL muscles were placed in Recovery buffer for 60 min at 35°C, then rinsed for 10 min at 29°C in 2 ml of oxygenated Krebs Henseleit Buffer (KHB) containing 40 mM mannitol to remove glucose from the extracellular space. After the rinse step, muscles were incubated for 20 min at 29°C in flasks containing 2 ml of KHB with 1mM 2-deoxy-[1,2-3H] glucose (2-DG; 1.5 μCi/ml) and 36 mM [14C] mannitol (0.2 μCi/ml), with a gas phase of 95% O_2-5% CO_2, in a shaking incubator. The same additions that were in the rinse were present during the determination of glucose transport. The muscles were then blotted and clamp frozen and processed for determination of intracellular 2-DG accumulation and extracellular space, as described previously (11, 45). 2-Deoxy-[1,2-3H] glucose was purchased from American Radiolabeled Chemicals (St. Louis, MO). [14C] mannitol was obtained from ICN Radiochemicals (Irvine, CA).

Statistical analysis

Tissue morphology, quantitative PCR and Western blot expression data as well as glucose uptake were analyzed using an analysis of variance (ANOVA) with surgery and time (and insulin for the glucose uptake assay) as factors using JMP statistical software (version 10.0.0). When significant differences were detected in parameters, pairwise comparisons were run using the Tukey HSD method. Pairwise comparisons are reported in the running text of the results section. The level of significance was set at $p < 0.05$. Data are presented as means ± S.E.M. (n).

RESULTS

Tissue Weight and Morphology

There was a significant effect of time and surgery on weight of GC and TA as well as a significant effect of surgery on SOL muscles (ANOVA, see Table 1 for all ANOVA p-values). The interaction between surgery and time was also significant for all three muscles ($p < 0.05$). There was not a significant difference in weight for any of the three muscles taken from the sham surgery limbs at any time point. Pairwise comparison revealed that transection surgery did not cause differences in muscle weight at three days post-surgery. By 10 days however, the muscle weight (as a percentage of body weight) of the SOL, GC, and TA was significantly lower in the transected limbs as compared to sham surgery ($p < 0.05$; Figure 2.1). Weight of the GC was lower still at 28 days, and did not change thereafter, while weight remained constant for the SOL and TA after day 10 ($p < 0.05$; Figure 2.1).

ANOVA revealed that time and surgery each had a significant effect on percent fibrotic area and myocyte cross-sectional area (CSA), ($p < 0.05$). Histological analysis via Gomori trichrome staining showed that the transected muscles had significantly greater fibrotic area (green coloration - indicating an increase in interstitial collagen) than sham surgery ($p < 0.05$; Figure 2.2A & 2.2C). Concordantly, the mean CSA was significantly lower ($p < 0.05$; Figure 2.2A & 2.2B) in the transected muscles.

Expression of Metabolic Genes

We investigated genes that are involved in regulation of metabolic function and found that time had a significant effect on gene expression for PPARδ and PGC-1β, with surgery having an effect on PPARα, PPARβ, PGC-1α, and PGC-1β ($p < 0.05$). The only significant interaction between time and surgery was for the expression of PGC-1β ($p < 0.05$). There was no significant difference in the expression levels for any of these genes at any time point in the sham surgery muscles ($p > 0.05$; Figure 2.3). PPARα, PPARδ, and PGC-1α expression after transection was significantly lower at all time points as compared to sham surgery ($p < 0.05$; Figure 2.3). Although later to develop, muscle from the transected limbs showed a significant decrease in the expression of PGC-1β at 10, 28, and 56 days post-surgery ($p < 0.05$; Figure 2.3). Surgery also led to significantly lower

expression levels of genes expressing metabolic enzymes (MCAD, MCPT1, CD36, PFK, and CS) in the transected muscles ($p < 0.05$) and none showed a significant interaction effect ($p > 0.05$); Figure 2.4).

Functional Glucose Uptake and Glucose Transporter Expression

There was a significant effect of time, surgery and their interaction on glucose uptake ($p < 0.05$). The functional glucose uptake assay performed on the EDL muscle demonstrated a blunted response to insulin stimulation in the transected muscles at 3 days post-surgery, but an increase in insulin response at 28 and 56 days post-surgery ($p < 0.05$; Figure 2.5). Pairwise comparison showed that basal glucose uptake was significantly higher at 28 and 56 days post-surgery ($p < 0.05$; Figure 2.5).

There was a significant effect of surgery on the gene expression of GLUT4, while there was a significant effect of surgery, time and their interaction on GLUT4 protein expression ($p < 0.05$). Although not significant, GLUT1 mRNA was lower in both sham and transected muscle at 56 days post-surgery. Pairwise comparison revealed that the GLUT4 protein expression was unchanged at 3 and 10 days in transected muscles but was significantly higher by 28 and 56 days post-surgery ($p < 0.05$; Figure 2.5). However, gene expression levels for GLUT4 at all time points were significantly lower in the transected muscles ($p < 0.05$; Figure 2.5). GLUT1 gene expression was not affected by any factors, but GLUT1 protein expression was significantly affected by surgery ($p < 0.05$). GLUT1 protein expression was significantly greater post transection surgery, although the effect was small ($p < 0.05$; Figure 2.5).

Akt Signaling

Surgery had a significant effect on protein expression of Akt2 ($p < 0.05$) with greater Akt2 protein expression post-surgery ($p < 0.05$; Figure 2.6). Surgery also had the significant effect of higher Akt phosphorylation after transection. There was no difference in the expression of AS160 or p-AS160 at any of the time points (data not shown).

DISCUSSION

This is the first report of the response of the muscle glucose uptake system following long-term denervation. The effects of denervation on skeletal muscle are wide-ranging and include significant atrophy of muscle mass. In their review, Thomason and Booth (34) noted that decreases in muscle mass are significant the first several weeks following surgery, but this rapid loss slows approximately 25-30 days post-surgery. This is significant to our study as previous investigations that noted decrements in glucose uptake were limited to shorter time courses (4, 7, 13, 25, 37). The observation that decreases in muscle mass were not noted after 25 days of disuse atrophy led to our hypothesis that the inhibition of glucose uptake seen in previous short-term denervation studies may not have been representative of the effects that chronic disuse atrophy has on glucose uptake. Previous research does not indicate changes in fiber type following prolonged transection in predominantly fast muscle (5,6). The EDL, TA & GC are primarily "fast" muscles and so few changes in fiber type should be expected. Additionally, we saw no evidence of change to a more oxidative fiber-type as demonstrated by our metabolic gene expression data.

In our study, denervation of the sciatic nerve decreased muscle mass in soleus by 27% and 41% by 10 days and 56 days post-surgery respectively, values that are quite similar to those previously reported (36). The sciatic nerve is both motor and sensory and innervates most of the hind-limb muscles. Although greater in scope, reductions in mass by 10 and 56 days post-surgery of tibialis anterior (40% and 59%) and gastrocnemius (50% and 68%) are also similar to those reported previously (5). Furthermore, and in agreement with earlier reports (5), we reported no differences in mass between 28 and 56-days post surgery. As there were no changes in mass for any of the sham surgery muscles over the course of the study, differences in mass could be accounted for as atrophy, not arrested development. The loss of mass was explained by reductions in mean myocellular CSA, which became significant 10 days post-surgery. Similar reductions in mean CSA following denervation have been reported in skeletal muscle (6, 39) and diaphragm muscle (2). Reductions in mean CSA were accompanied by increases in tissue fibrosis area, an effect of denervation or immobilization that has also been demonstrated

previously (3, 29, 43). Previous studies had focused on changes in glucose uptake shortly after surgery (3 hours to 17 days post-surgery), a period when apoptotic and necrotic pathways are most active. However, our data demonstrate that by 28 days post-surgery, there was little evidence for activity of these pathways by the plateau in loss of muscle mass. Therefore, we investigated changes in glucose uptake to determine if there were indeed compensatory responses once apoptotic and necrotic activity had slowed significantly.

Following denervation surgery, decrements in insulin-stimulated glucose uptake have been noted as quickly as 3 hours, although maximal effects were often not noted for 3 days (4, 7, 13, 25, 37). Similarly, it has also been shown that between 3 days and 17 days post-surgery, there was no change in the decrement in insulin-stimulated glucose uptake caused by denervation of the gastrocnemius muscle (36). Results from our functional glucose uptake assay show that glucose uptake in earlier time points (3 days post-surgery) was unchanged in denervated tissues. However, by 28 and 56 days post-surgery, insulin stimulated glucose uptake was greater in denervated muscles than in sham-surgery tissues. Likewise, basal glucose uptake was initially unaffected by denervation surgery, but was 2-fold higher in the 28 and 56 day groups. To determine the mechanisms responsible for the improved glucose uptake, we investigated glucose transporters and components of the insulin-signaling pathway.

The expression of GLUT4 protein mirrored the changes in glucose uptake throughout our time course. The initially lower mRNA & protein expression (although not significant for protein) of GLUT4 at 3 days post-transection were similar to those noted previously (4, 7, 16). GLUT4 mRNA remained low throughout the experiment; however, GLUT4 protein expression in denervated muscles was significantly greater at the 28 and 56-day time points. These results are similar to those reported previously, which showed that in late-stage streptozotocin induced diabetes, there are decreases in GLUT4 protein, but in the early stages GLUT4 protein levels are unchanged (17). Therefore, it is possible that the diabetic phenotype was nascent in our model. Additionally, the decreases in GLUT4 mRNA without changes in GLUT4 protein expression suggest that the turnover of protein is slower than that of mRNA.

It has been shown previously that Akt plays a key role in glucose homeostasis;

decreases in glucose uptake 24 hours after denervation were attributed to decreases in Akt activation, as GLUT4 protein expression was unchanged (13, 42). Furthermore, over-expression of Akt in adipocytes from rats caused an increase in GLUT4 translocation, independent of insulin (8). In our study, both Akt2 and GLUT4 protein expression were increased in response to transection. Basal glucose uptake was also increased in the later time points in denervated muscles, although GLUT1 expression was unchanged. Via increased Akt activation, it has been shown in several cell lines that cytokines or other growth factors are able to increase basal glucose uptake by increased recycling of GLUT1 vesicles and promotion of cell surface integration without a change in GLUT1 protein levels (41, 44). The increased expression of both GLUT4 and Akt2 protein noted in the later time points, in concert with the increased insulin-stimulated glucose uptake seen at the later time points in our study further reinforces the idea that compensatory mechanisms involving the insulin-signaling pathway act to restore the capacity for glucose uptake in response to long-term disuse atrophy. Although we did not measure the translocation of GLUT4, it is possible that some unknown mechanism could have increased the localization of GLUT4 to the membrane, which could allow for higher glucose uptake.

The restoration of glucose uptake at later time points was cause for investigation into the effects that long-term denervation had on other metabolic pathways and on regulators of metabolism. The peroxisome proliferator-activated receptors (PPARα and PPARδ) and their co-activators (PGC-1α and PGC-1β) are known regulators of both lipid and glucose metabolism as well as mitochondrial biogenesis. PPARδ has been shown to be strongly linked to glucose homeostasis; in human myotubes, PPARδ agonists increased glucose metabolism (20), while in *ob/ob* mice, pharmacological enhancement of PPARδ activation improved glucose sensitivity and insulin response (34). Additionally, mice lacking the PPARδ gene were glucose intolerant (21). PGC-1β has also been shown to affect glucose homeostasis, as transgenic mice overexpressing PGC-1β were lighter and had lower plasma insulin levels than pair matched controls when fed a high fat diet (17). However, the effect that PGC-1α has on insulin resistance in obese mice is unclear as transgenic mice overexpressing PGC-1α were more insulin resistant and showed decreases in GLUT4 mRNA (26) while PGC-1α null mice demonstrated

improvements in glucose uptake and insulin response (24).

The effects of long-term denervation on these metabolic regulators are less understood. Long-term denervation (42 days) in rats was shown to decrease PGC-1α expression by 70% (1). In mice, PGC-1α and PGC-1β expression were decreased by 80% and 42% respectively 30 days after surgery (38). In our study the expression levels for PPARα, PPARδ, PGC-1α, and PGC-1β were all decreased by ~ 50 % from day 10 through day 56. These data indicate that these regulators of metabolism are down-regulated by denervation and do not appear to recover. There does not appear to be a direct connection between these metabolic regulators and the restoration of insulin sensitivity, although this appears to be in direct opposition to most studies, which show a strong correlation between metabolic regulation and glucose uptake. For example, it has been shown in muscle-specific knockout mice lacking the PGC-1α gene that caloric restriction was able to improve glucose homeostasis (10). Therefore, although there is a close relationship between these metabolic regulators and glucose homeostasis, other mechanisms (such as the increase in GLUT4 expression, and perhaps localization at the cell membrane, and Akt2 expression) appear able to compensate for the drop in expression with disuse atrophy.

The discrepancy between metabolic regulation and glucose uptake led us to investigate the effect that denervation would have on genes regulating enzymes involved in fatty acid transport and glycolysis. Due to the strong effect that PPARα, PPARδ, PGC-1α, and PGC-1β have on glucose and lipid metabolism and the observed reductions in their gene expression, it was not surprising that the expression profile for MCAD, M-CPT1, CD36, and CS followed similar patterns. Similar to glucose uptake, transport of fatty acids into skeletal muscle responds to changes in muscle contraction or insulin levels, and studies have shown an association between ineffective fatty acid transport and metabolic pathologies (12, 15, 33). Although the effects of long-term denervation on fatty acid transport are unknown, 7 days of disuse atrophy following denervation surgery (19) increased palmitate uptake, although FAT/CD36 protein expression was unchanged. It was not surprising that the lower expression for these genes involved in fatty acid transport and glycolysis did not have an effect on glucose uptake.

To our knowledge, this is the first report of the effects that long-term denervation

has on functional glucose uptake. We demonstrated that both basal and insulin stimulated glucose uptake in transected muscles were greater than control at 56 days post-surgery. This is especially interesting given that the expression of the metabolic genes in transected muscles was not restored, with the difference being especially notable in later time points. Although the exact mechanisms for the improvement in glucose uptake are unclear at this time, it appears that the greater protein expression we noted for both GLUT4 and Akt2 shown in transected muscles are partially responsible. Although GLUT4 protein was increased, it is possible that other mechanisms, such as increased translocalization of GLUT4 to the plasma membrane, increased fusion with the plasma membrane, or functional activity of GLUT4 are responsible for the increase in glucose uptake. Further inquiries into the mechanisms underlying this response are clearly warranted.

REFERENCES

1. Adhihetty PJ, O'Leary MFN, Chabi B, Wicks KL, Hood DA. Effect of denervation on mitochondrially mediated apoptosis in skeletal muscle. *Journal of Applied Physiology* 102: 1143–1151, 2007.
2. Aravamudan B, Mantilla CB, Zhan W-Z, Sieck GC. Denervation effects on myonuclear domain size of rat diaphragm fibers. *Journal of Applied Physiology* 100: 1617–22, 2006.
3. Arruda EM, Mundy K, Calve S, Baar K. Denervation does not change the ratio of collagen I and collagen III mRNA in the extracellular matrix of muscle. *American Journal of Physiology Regulatory Integrative and Comparative Physiology* 292: R983–R987, 2007.
4. Block NE, Menick DR, Robinson KA, Buse MG. Effect of denervation on the expression of two glucose transporter isoforms in rat hindlimb muscle. *The Journal of Clinical Investigation* 88: 1546–52, 1991.
5. Booth FW. Time course of muscular atrophy during immobilization of hindlimbs in rats. *Journal of Applied Physiology* 43: 656–661, 1977.
6. Borisov AB, Dedkov EI, Carlson BM. Interrelations of Myogenic Response, Progressive Atrophy of Muscle Fibers, and Cell Death in Denervated Skeletal Muscle. *Anatomical Records* 218: 203–218, 2001.
7. Coderre L, Monfar MM, Chen KS, Heydrick SJ, Kurowski TG, Ruderman NB, Pilch PF. Alteration in the expression of GLUT-1 and GLUT-4 protein and messenger RNA levels in denervated rat muscles. *Endocrinology* 128: 1821–1825, 1991.
8. Cong LN, Chen H, Li Y, Zhou L, McGibbon M a, Taylor SI, Quon MJ. Physiological role of Akt in insulin-stimulated translocation of GLUT4 in transfected rat adipose cells. *Molecular Endocrinology* 11: 1881–90, 1997.
9. Danaei G, Finucane MM, Lu Y, Singh GM, Cowan MJ, Paciorek CJ, Lin JK, Farzadfar F, Khang Y-H, Stevens G a, Rao M, Ali MK, Riley LM, Robinson CA, Ezzati M. National, regional, and global trends in fasting plasma glucose and diabetes prevalence since 1980: systematic analysis of health examination surveys and epidemiological studies with 370 country-years and 2·7 million participants. *Lancet* 378: 31–40, 2011.
10. Finley LWS, Lee J, Souza A, Desquiret-Dumas V, Bullock K, Rowe GC, Procaccio V, Clish CB, Arany Z, Haigis MC. Skeletal muscle transcriptional coactivator PGC-1α mediates mitochondrial, but not metabolic, changes during calorie restriction. *Proceedings of the National Academy of Sciences of the United States of America* 109: 2931–6, 2012.

11. Geiger PC, Han DH, Wright DC, Holloszy JO. How muscle insulin sensitivity is regulated: testing of a hypothesis. *American Journal of Physiology Regulatory Integrative and Comparative Physiology* 291:E1258-1263, 2006.

12. Glatz J, Luiken J, Bonen A. Membrane fatty acid transporters as regulators of lipid metabolism: implications for metabolic disease. *Physiological Reviews*. 2010.

13. Henriksen EJ, Rodnick KJ, Mondon CE, James DE, Holloszy JO. Effect of denervation or unweighting on GLUT-4 protein in rat soleus muscle. *Journal of Applied Physiology* 70: 2322–2327, 1991.

14. Ivy JL, Young JC, McLane JA, Fell RD, Holloszy JO. Exercise training and glucose uptake by skeletal muscle in rats. *Journal of Applied Physiology* 55: 1393–1396, 1983.

15. Jain SS, Chabowski A, Snook LA, Schwenk RW, Glatz JFC, Luiken JJFP, Bonen A. Additive effects of insulin and muscle contraction on fatty acid transport and fatty acid transporters, FAT/CD36, FABPpm, FATP1, 4 and 6. *FEBS Letters* 583: 2294–300, 2009.

16. Jensen EB, Zheng D, Russell RA, Bassel-Duby R, Williams RS, Olson AL, Dohm GL. Regulation of GLUT4 expression in denervated skeletal muscle. *American Journal of Physiology. Regulatory, Integrative and Comparative Physiology* 296: R1820–8, 2009.

17. Kahn BB, Rossetti L, Lodish HF, Charron MJ. Decreased in vivo glucose uptake but normal expression of GLUT1 and GLUT4 in skeletal muscle of diabetic rats. *J Clin Invest*. 87: 2197–2206, 1991

18. Kamei Y, Ohizumi H, Fujitani Y, Nemoto T, Tanaka T, Takahashi N, Kawada T, Miyoshi M, Ezaki O, Kakizuka A. PPARγ coactivator 1β/ERR ligand 1 is an ERR protein ligand, whose expression induces a high-energy expenditure and antagonizes obesity. *Proceedings of the National Academy of Sciences of the United States of America* 100: 12378–12383, 2003.

19. Klip A, Pâquet MR. Glucose transport and glucose transporters in muscle and their metabolic regulation. *Diabetes Care* 13: 228–43, 1990.

20. Koonen DPY, Benton CR, Arumugam Y, Tandon NN, Calles-Escandon J, Glatz JFC, Luiken JJFP, Bonen A. Different mechanisms can alter fatty acid transport when muscle contractile activity is chronically altered. *American Journal of Physiology. Endocrinology and Metabolism* 286: E1042–9, 2004.

21. Kramer HF, Witczak CA, Taylor EB, Fujii N, Hirshman MF, Goodyear LJ. AS160 regulates insulin- and contraction-stimulated glucose uptake in mouse skeletal muscle. *The Journal of Biological Chemistry* 281: 31478–85, 2006.

22. Latouche C, Jowett JBM, Carey AL, Bertovic DA, Owen N, Dunstan DW, Kingwell BA. Effects of Breaking up Prolonged Sitting on Skeletal Muscle Gene Expression. *Journal of Applied Physiology*: 453–460, 2012.

23. Lee C-H, Olson P, Hevener A, Mehl I, Chong L-W, Olefsky JM, Gonzalez FJ, Ham J, Kang H, Peters JM, Evans RM. PPARdelta regulates glucose metabolism and insulin sensitivity. *Proceedings of the National Academy of Sciences of the United States of America* 103: 3444–3449, 2006.

24. Lees SJ, Frank W. Sedentary Death Syndrome Introduction: Inactivity is an Actual Cause of Death. *Canadian Journal of Applied Physiology*. 29: 447–460, 2004.

25. Lin J, Wu P-H, Tarr PT, Lindenberg KS, St-Pierre J, Zhang C-Y, Mootha VK, Jäger S, Vianna CR, Reznick RM, Cui L, Manieri M, Donovan MX, Wu Z, Cooper MP, Fan MC, Rohas LM, Zavacki AM, Cinti S, Shulman GI, Lowell BB, Krainc D, Spiegelman BM. Defects in adaptive energy metabolism with CNS-linked hyperactivity in PGC-1alpha null mice. *Cell* 119: 121–35, 2004.

26. Megeney LA, Neufer PD, Dohm GL, Tan MH, Blewett CA, Elder GC, Bonen A. Effects of muscle activity and fiber composition on glucose transport and GLUT-4. *American Journal of Physiology* 264: E583–E593, 1993.

27. Miura S, Kai Y, Ono M, Ezaki O. Overexpression of peroxisome proliferator-activated receptor gamma coactivator-1alpha down-regulates GLUT4 mRNA in skeletal muscles. *The Journal of Biological Chemistry* 278: 31385–90, 2003.

28. O'Rahilly S. Diabetes in midlife: Planting genetic time bombs. *Nature Methods* 3: 1080–1081, 1997.

29. Pessin JE, Saltiel AR. Signaling pathways in insulin action: molecular targets of insulin resistance. *Journal of Clinical Investigations:* 165–169, 2000.

30. Salonen V, Lehto M, Kalimo M, Penttinen R, Aro H. Changes in intramuscular collagen and fibronectin in denervation atrophy. *Muscle Nerve* 8: 125–131, 1985.

31. Shaw JE, Sicree R a, Zimmet PZ. Global estimates of the prevalence of diabetes for 2010 and 2030. *Diabetes Research and Clinical Practice* 87: 4–14, 2010.

32. Shulman GI. Cellular mechanisms of insulin resistance. *Journal of Clinical Investigations* 106: 171–176, 2000.

33. Sigal RJ, Kenny GP, Wasserman DH, Castaneda-Sceppa C, White RD. Physical activity/exercise and type 2 diabetes: a consensus statement from the American Diabetes Association. *Diabetes Care* 29: 1433–8, 2006.

34. Talanian JL, Holloway GP, Snook LA, Heigenhauser GJF, Bonen A, Spriet LL. Exercise training increases sarcolemmal and mitochondrial fatty acid transport proteins in human skeletal muscle. *American Journal of Physiology. Endocrinology and Metabolism* 299: E180–8, 2010.

35. Tanaka T, Yamamoto J, Iwasaki S, Asaba H, Hamura H, Ikeda Y, Watanabe M, Magoori K, Ioka RX, Tachibana K, Watanabe Y, Uchiyama Y, Sumi K, Iguchi H, Ito S, Doi T, Hamakubo T, Naito M, Auwerx J, Yanagisawa M, Kodama T, Sakai J. Activation of peroxisome proliferator-activated receptor δ induces fatty acid ␣-oxidation in skeletal. *Proceedings of the National Academy of Sciences of the United States of America;100:15924-9*. 2003.

36. Thomason DB, Booth FW. Atrophy of the soleus muscle by hindlimb unweighting. *Journal of Applied Physiology* 68193: 1–12, 1990.

37. Thomason DB, Herrick RE, Surdyka D, Baldwin KM. Time course of soleus muscle myosin expression during hindlimb suspension and recovery. *Journal of Applied Physiology* 63: 130–137, 1987.

38. Turinsky J. Dynamics of insulin resistance in denervated slow and fast muscles in vivo. *Am J Physiol Regulatory Integrative Comp Physiol* 252: 531–537, 1987.

39. Wagatsuma A, Kotake N, Mabuchi K, Yamada S. Expression of nuclear-encoded genes involved in mitochondrial biogenesis and dynamics in experimentally denervated muscle. *Journal of Physiology and Biochemistry* 67: 359–370, 2011.

40. Wagatsuma A. Upregulation of gene encoding adipogenic transcriptional factors C/EBPalpha and PPARgamma2 in denervated muscle. *Experimental Physiology* 91: 747–753, 2006.

41. Watson RT, Pessin JE. Intracellular organization of insulin signaling and GLUT4 translocation. *Recent Progress in Hormone Research* 56: 175–93, 2001.

42. Wieman HL, Wofford JA, Rathmell JC. Cytokine Stimulation Promotes Glucose Uptake via Phosphatidylinositol-3 Kinase / Akt Regulation of Glut1 Activity and Trafficking. *Molecular Biology of the Cell* 18: 1437–1446, 2007.

43. Wilkes JJ, Bonen A. Reduced insulin-stimulated glucose transport in denervated muscle is associated with impaired Akt-alpha activation. *American Journal of Physiology - Endocrinology And Metabolism* 279: E912–E919, 2000.

44. Williams PE, Goldspink G. Connective tissue changes in immobilised muscle. *Journal of Anatomy* 138: 343–350, 1984.

45. Wofford J a, Wieman HL, Jacobs SR, Zhao Y, Rathmell JC. IL-7 promotes Glut1 trafficking and glucose uptake via STAT5-mediated activation of Akt to support T-cell survival. *Blood* 111: 2101–11, 2008.

46. Young DA, Uhl JJ, Cartee GD, Holloszy JO Activation of Glucose Transport in Muscle by Prolonged Exposure to Insulin. *Journal of Biological Chemistry* 261:16049-16053, 1986.

TABLES

Table 2.1 Primer sequences for qPCR

Gene	Forward	Reverse
PPARα	ACTACGGAGTTCACGCATGTG	TTGTCGTCAACCAGCTTCAGC
PPARδ	TCACCGGCAAGTCCAGCC	ACACCAGGCCCTTCTCTGGCT
PGC-1α	CGGAAATCATATCCAACCAG	TGAGGACCACTAGCAAGTTG
PGC1β	TCCAGAAGTCAGCGGCCT	CTGAGCCCGCAGTGTGG
MCAD	GGCTCCTGAGAAGTGTTTCTC	GGCTCCTGGTTGTGAGC
MCPT1	TCTAGGGAATGCCGTTCAC	GAGCACATGGGCACCATAC
CD36	CAAGCTCCTTGGCATGGTAGA	TGGATTTGCAAGCACAATATA
PFK	CGTTGAGGTAGGAATACTTCTA	ACCTCTTCCGAAAGGAGTGA
CS	CAAGCAACATGGGAAGA	GTCAGGAAGAACCGAAGTCT
GLUT4	ATCATCCGGAACCTGGAGG	GTCAGACACATCAGCCGAGC
GLUT1	TCGTTGGCATCCTTATTGC	ACGAAGACGACACTGAGCAG
36B4	AGATGCAGCAGATCCGCAT	ATATGAGGCAGCAGTTTCTCG

FIGURE LEGENDS

Figure 2.1 Denervation leads to rapid initial weight loss in hind-limb muscles with no subsequent loss after 28 days post surgery. A. Soleus B. Gastrocnemius C. Tibialis Anterior. Muscle weight is expressed as a percentage of body weight (n = 18 for each). Values are means ± SEM. Different superscripted letters indicate significant pairwise differences between groups following significant time by surgery interaction (ANOVA $p < 0.05$).

Figure 2.2 Myocellular cross-sectional area is reduced following denervation surgery. A. Representative images of fiber cross sectional sections stained with Gomori-trichrome. B. Myocellular cross-sectional area is lower in cross section of TA muscle with time (n = 5). C. Myocellular area exhibiting fibrosis is higher in denervation muscles (n = 5). Open bars represent sham surgery while closed bars represent denervation surgery. Values are means ± SEM, (n = 9 - 11). * indicates a significant effect of surgery (ANOVA $p < 0.05$).

Figure 2.3 mRNA expression is lower for genes involved in metabolic regulation in denervated GC muscle throughout time course of study. A. PPAR B. PPARδ; C. PGC-1 D. PGC-1. Open bars represent sham surgery while closed bars represent denervation surgery. Values are means ± SEM, (n = 9- 11). Quantitative data for each gene were normalized and corrected for the expression of a housekeeping gene (36B4). * indicates a significant effect of surgery (ANOVA $p < 0.05$). Different superscripted letters indicate significant pairwise differences between groups following significant time by surgery interaction (ANOVA $p < 0.05$).

Figure 2.4 mRNA expression is lower for genes regulating metabolic enzymes in denervated GC muscle throughout time course of study. A. MCAD; B. MCPT-1; C. CD36; D. PFK; E. CS. Open bars represent sham surgery while closed bars represent denervation surgery. Values are means ± SEM, (n = 9 - 11). Quantitative data for each gene were normalized and corrected for the expression of a housekeeping gene (36B4). * indicates a significant effect of surgery (ANOVA $p < 0.05$).

Figure 2.5 Skeletal muscle glucose uptake and transport improves in response to chronic denervation over the course of long-term denervation. 2-DG uptake is greater in chronically denervated EDL muscle. Sham (open bar), sham plus insulin (diagonal stripes), denervated (gray bar), denervated plus insulin (closed bar). Values are means ± SEM, (n = 7 - 9), $p < 0.05$. Significant pairwise differences between transected and sham surgery groups after insulin treatment is indicated by ♯. Significant pairwise differences between transected and sham surgery groups before insulin treatment is indicated by ≠.

Figure 2.6 A. GLUT4 protein expression is higher in chronically denervated GC muscle while GLUT4 gene expression is lower in chronically denervated GC muscle. B. GLUT1

protein expression is higher in chronically denervated GC muscle. GLUT1 gene expression is not different in chronically denervated GC muscle. Expression presented relative to 3-day sham. Ponceau S staining was used to verify loading volumes for Western blots. Values are means ± SEM, (n = 7 - 9). * indicates a significant effect of surgery (ANOVA $p < 0.05$). Different superscripted letters indicate significant pairwise differences between groups following significant time by surgery interaction (ANOVA $p < 0.05$). S = Sham, T = Transected.

Figure 2.7 The response of Akt2 to chronic denervation suggests compensation to maintain insulin signaling in GC muscle. A. Total Akt2 expression is higher in denervated muscle. B. Amount of phospho-Akt is higher with denervation surgery. Mice were injected with either insulin (0.5 U/mouse) or saline 10 minutes prior to sacrifice. Only insulin injected animals are shown. Open bars represent sham surgery while closed bars represent denervation surgery. Expression presented relative to 3-day sham. Ponceau S staining was used to verify loading volumes for Western blots. Values are means ± SEM, (n = 7 - 9). * indicates a significant effect of surgery (ANOVA $p < 0.05$). Different superscripted letters indicate significant pairwise differences between groups following significant time by surgery interaction (ANOVA $p < 0.05$).

FIGURES

Figure 2.1A

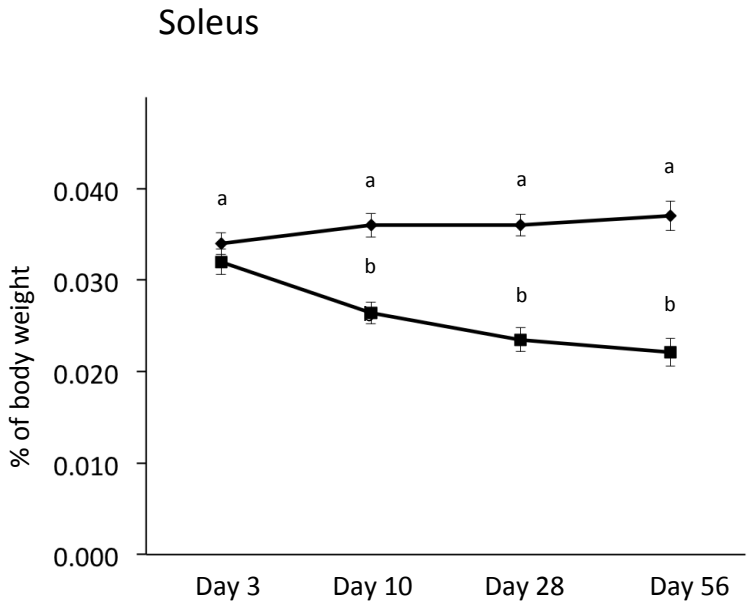

Figure 2.1B

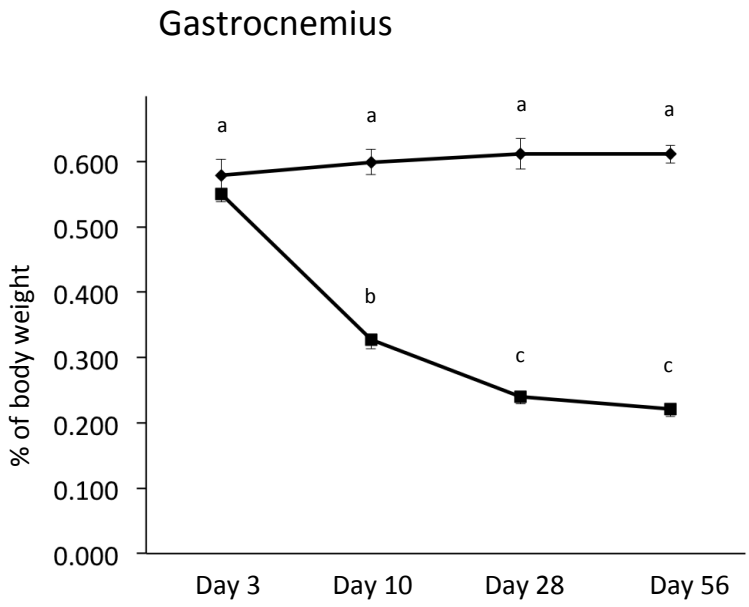
Gastrocnemius
% of body weight
0.600
0.500
0.400
0.300
0.200
0.100
0.000
a
a
a
a
b
c
c
Day 3
Day 10
Day 28
Day 56

Figure 2.1C

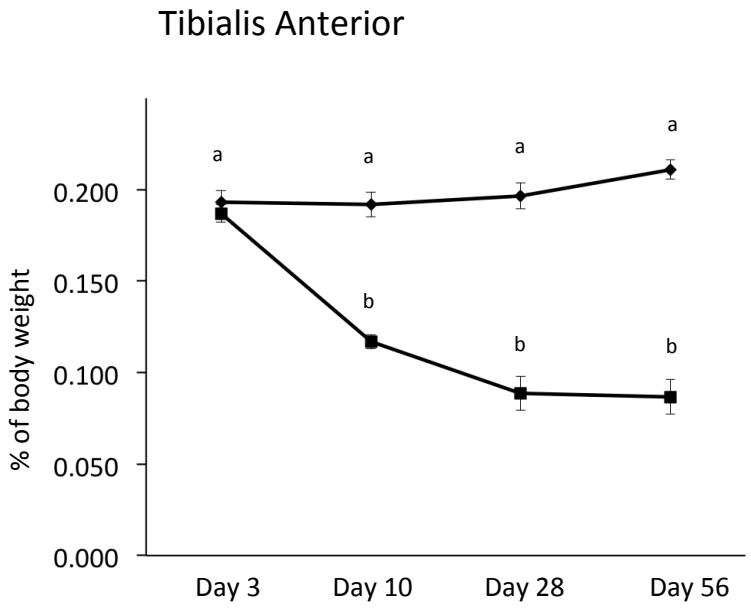
Tibialis Anterior
% of body weight
0.200
0.150
0.100
0.050
0.000
a
a
a
a
b
b
b
Day 3
Day 10
Day 28
Day 56

Figure 2.2A

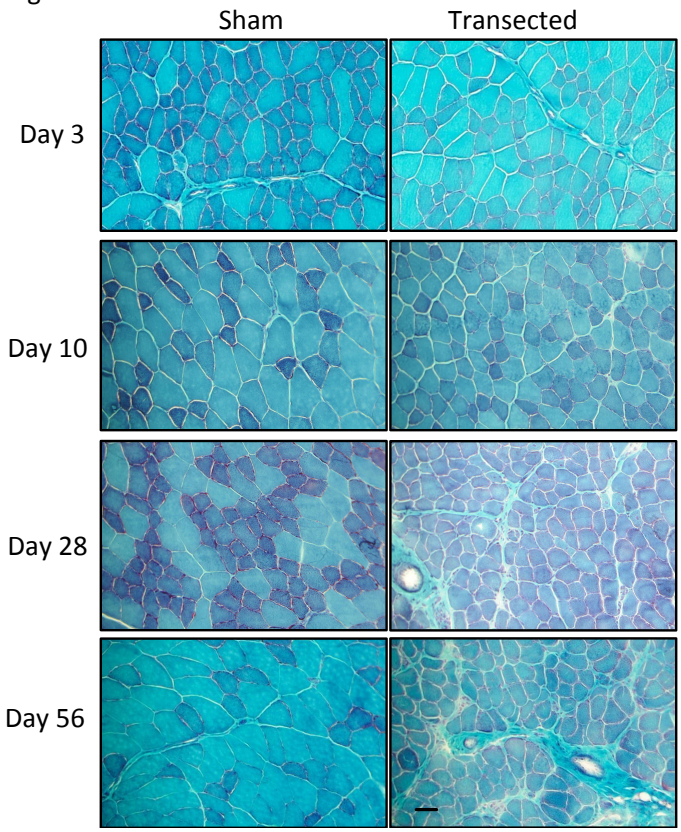

Figure 2.2B

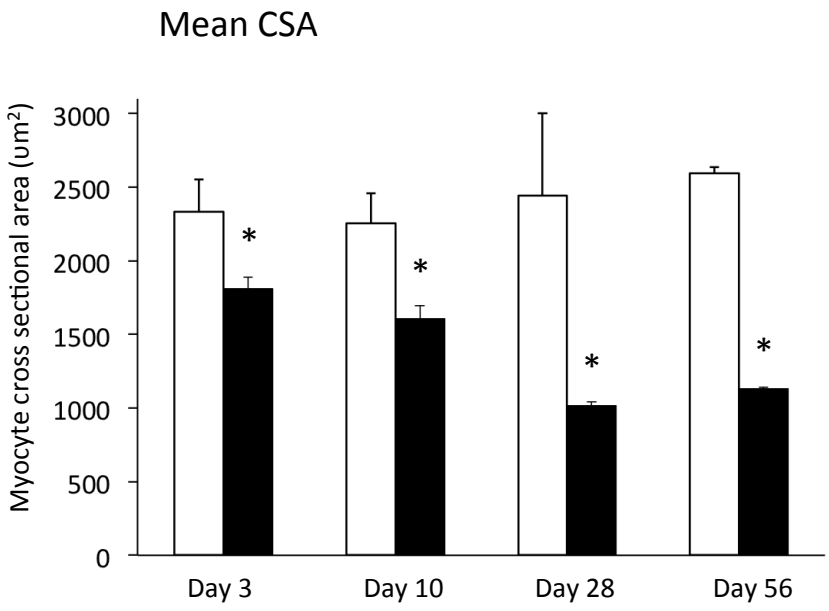
Mean CSA
Myocyte cross sectional area (um2)
3000
2500
2000
1500
1000
500
0
*
*
*
*
Day 3
Day 10
Day 28
Day 56

Figure 2.2C

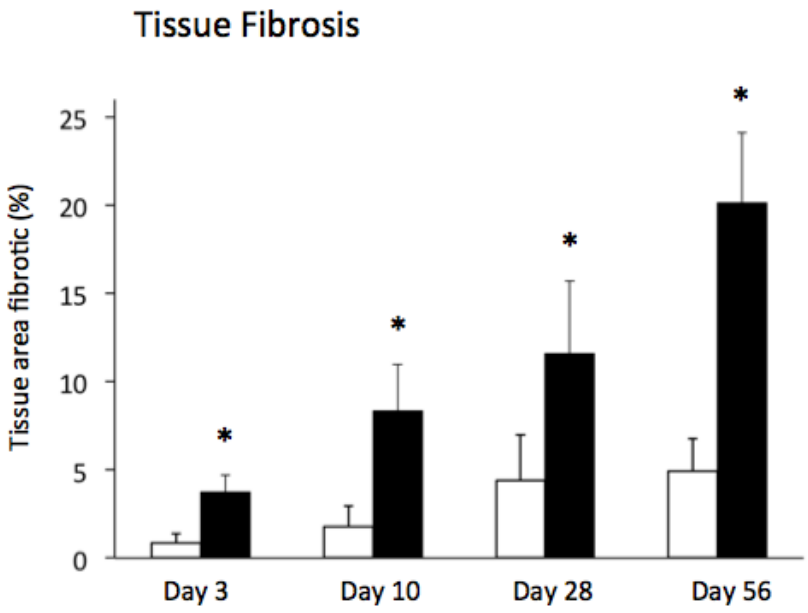
Tissue Fibrosis
Tissue area fibrotic (%)
25
20
15
10
5
0
*
*
*
*
Day 3
Day 10
Day 28
Day 56

Figure 2.3A

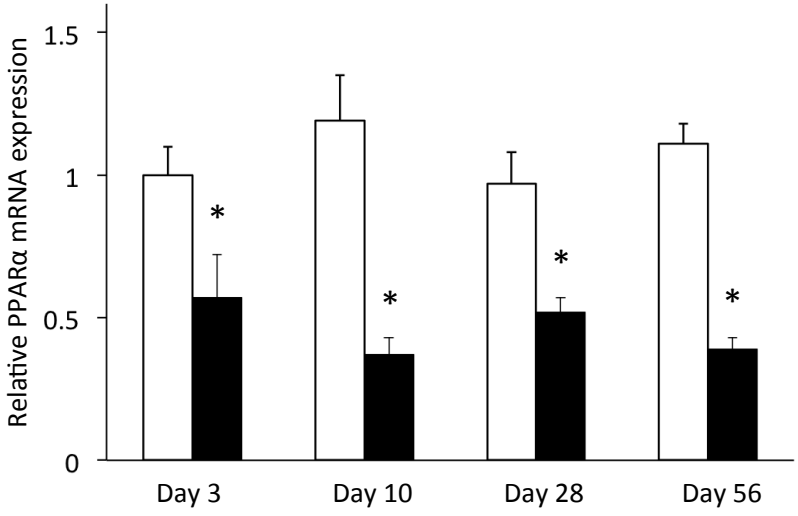
Relative PPARα mRNA expression
1.5
1
0.5
0
*
*
*
*
Day 3
Day 10
Day 28
Day 56

Figure 2.3B

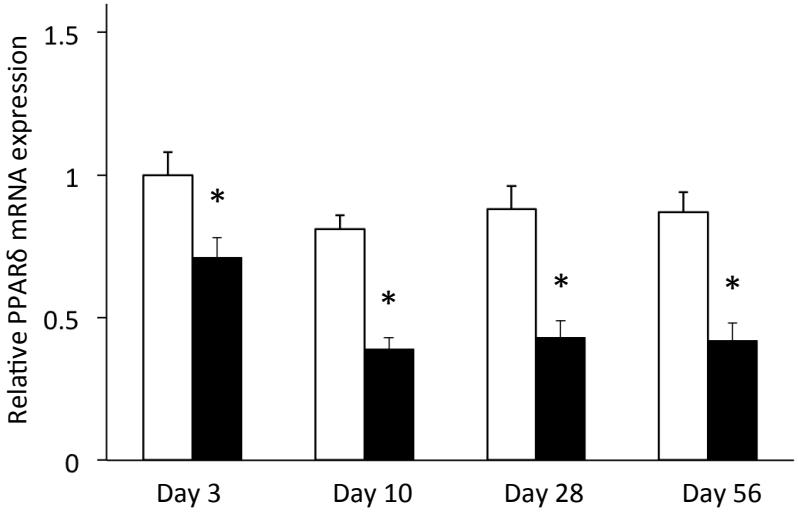
Relative PPARδ mRNA expression
1.5
1
0.5
0
*
*
*
*
Day 3
Day 10
Day 28
Day 56

Figure 2.3C

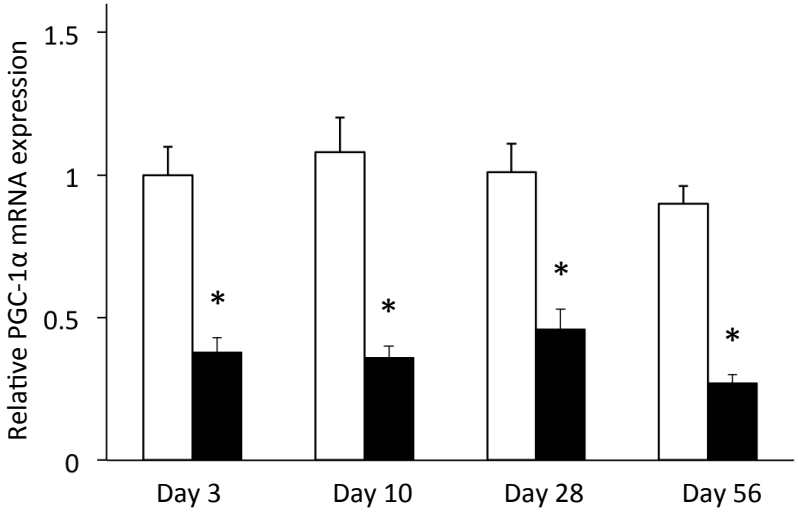
Relative PGC-1α mRNA expression
1.5
1
0.5
0
*
*
*
*
Day 3
Day 10
Day 28
Day 56

Figure 2.3D

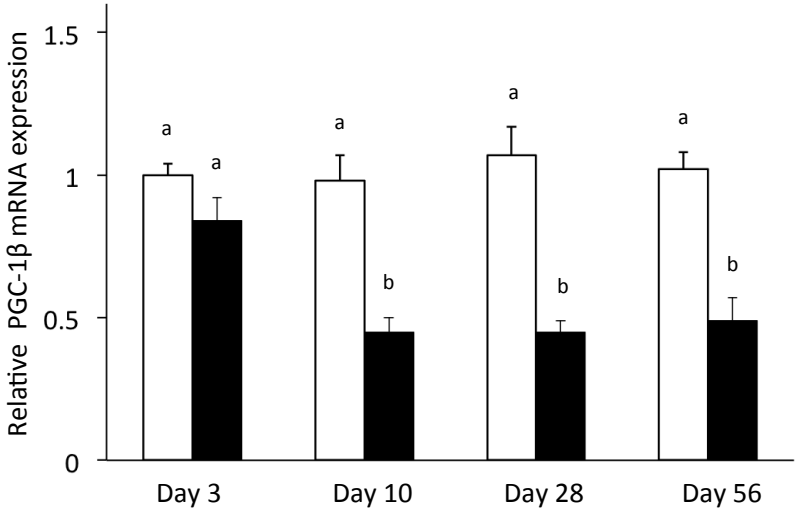
Relative PGC-1β mRNA expression
1.5
1
0.5
0
a
a
a
b
a
b
a
b
Day 3
Day 10
Day 28
Day 56

Figure 2.4A

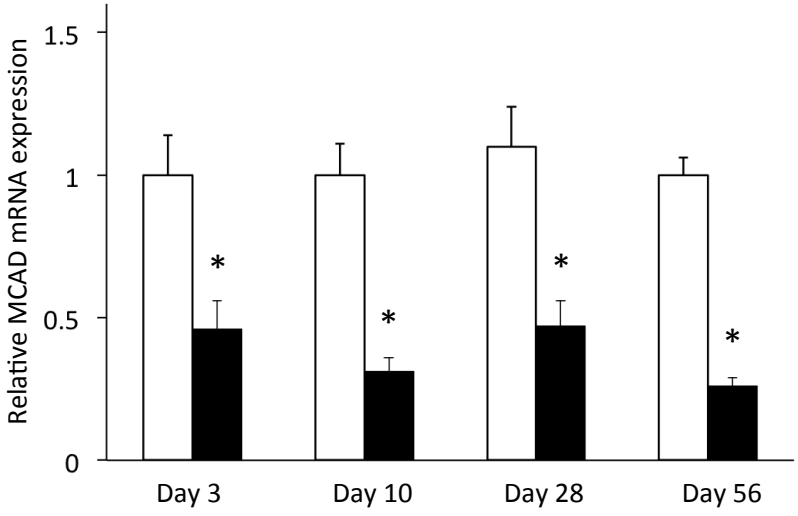
Relative MCAD mRNA expression
1.5
1
0.5
0
*
*
*
*
Day 3
Day 10
Day 28
Day 56

Figure 2.4B

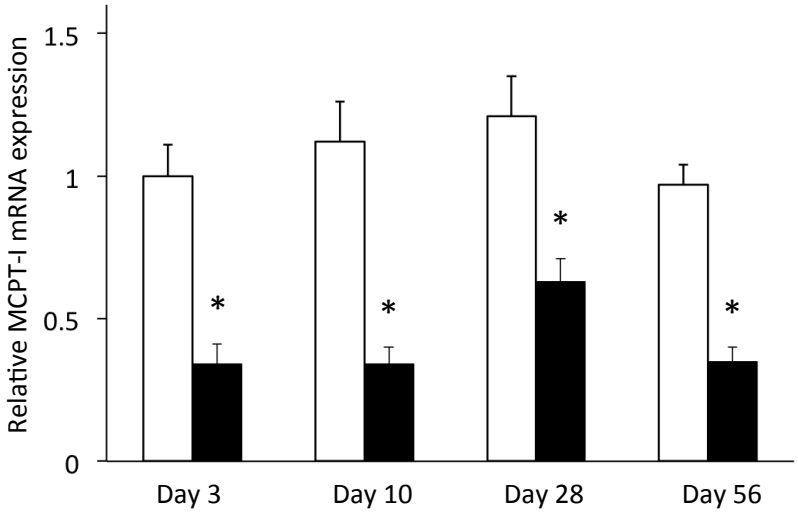
Relative MCPT-I mRNA expression
1.5
1
0.5
0
*
*
*
*
Day 3
Day 10
Day 28
Day 56

Figure 2.4C

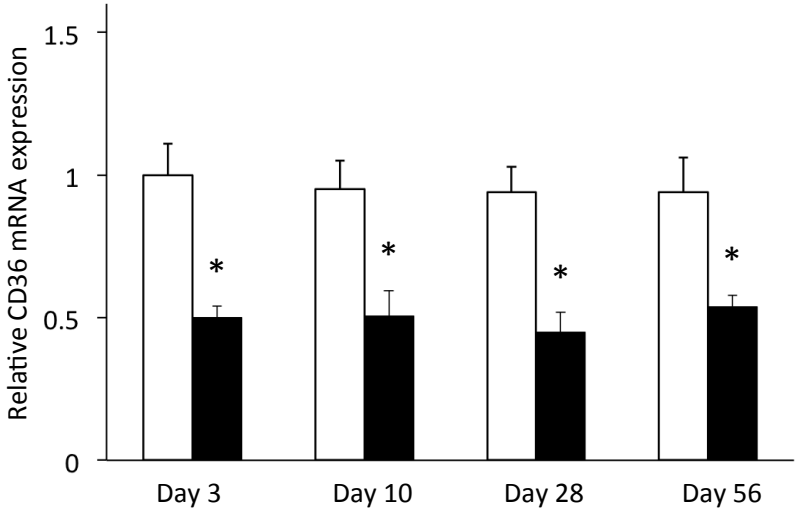
Relative CD36 mRNA expression
1.5
1
0.5
0
*
*
*
*
Day 3
Day 10
Day 28
Day 56

Figure 2.4D

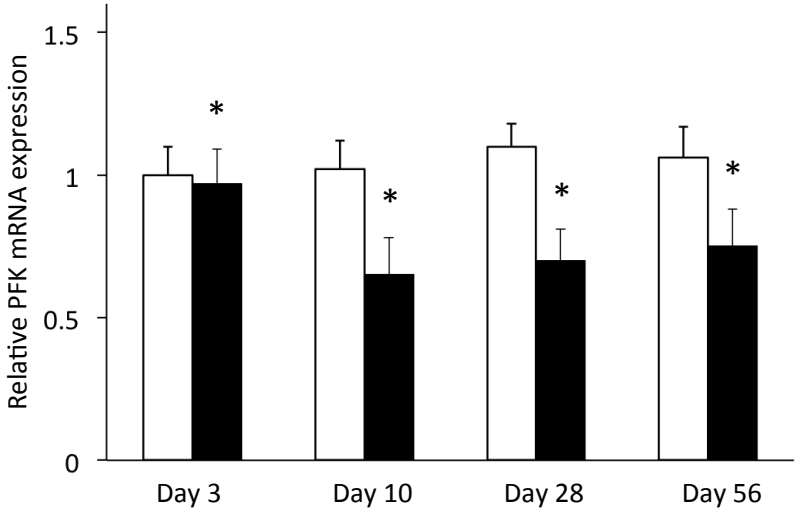
Relative PFK mRNA expression
1.5
1
0.5
0
*
*
*
*
Day 3
Day 10
Day 28
Day 56

Figure 2.4E

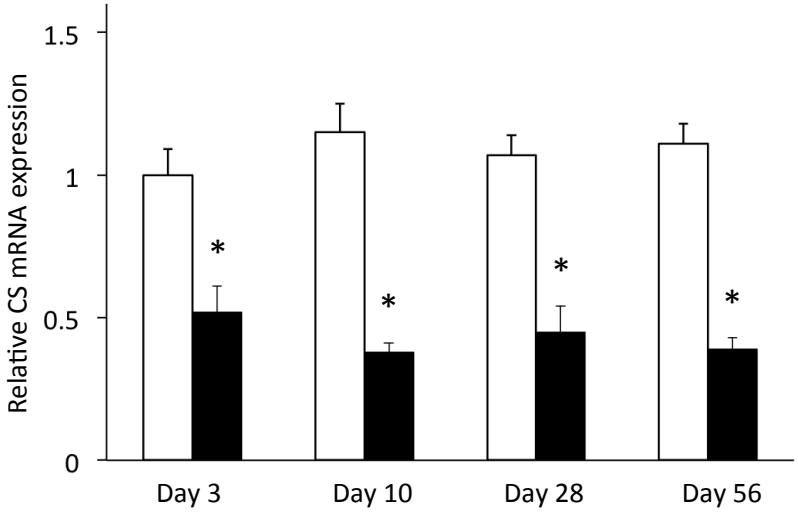

Figure 2.5

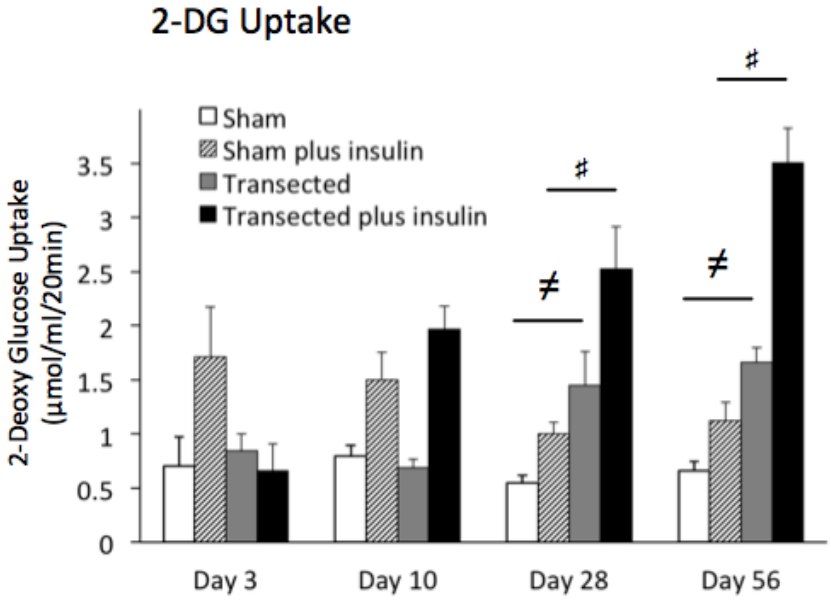
2-DG Uptake
Sham
Sham plus insulin
Transected
Transected plus insulin
2-Deoxy Glucose Uptake (µmol/ml/20min)
0
0.5
1
1.5
2
2.5
3
3.5
≠
♯
≠
♯
Day 3
Day 10
Day 28
Day 56

Figure 2.6A

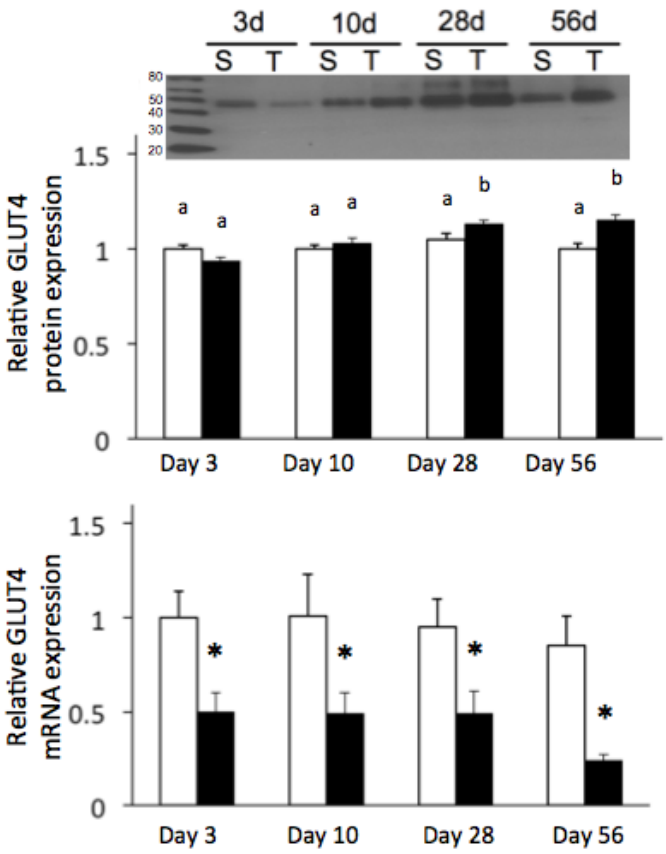
3d
10d
28d
56d
S T S T S T S T
80
50
40
30
20
Relative GLUT4 protein expression
1.5
1
0.5
0
a a a a a b a b
Day 3
Day 10
Day 28
Day 56
Relative GLUT4 mRNA expression
1.5
1
0.5
0
* * * *
Day 3
Day 10
Day 28
Day 56

Figure 2.6B

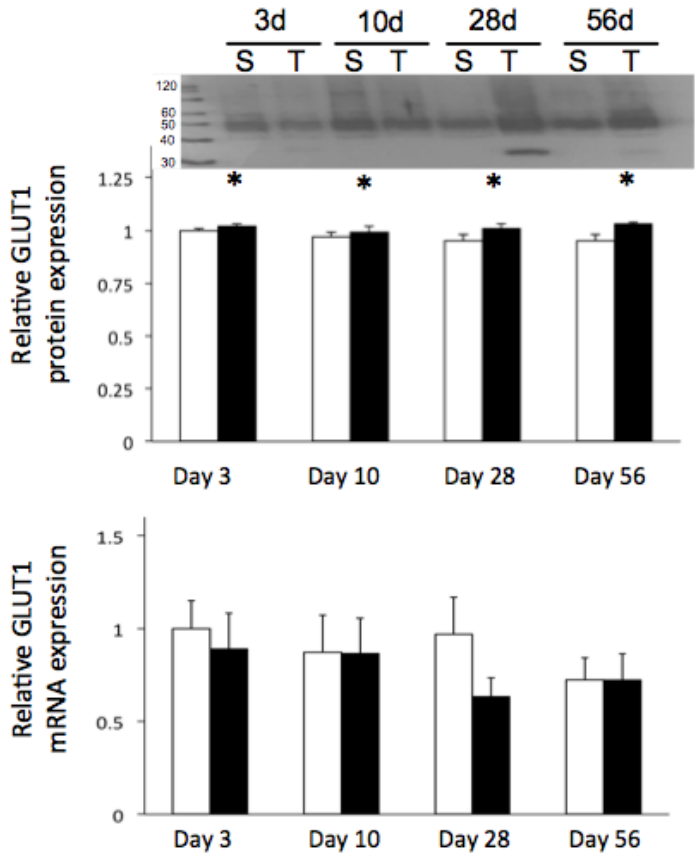
3d
10d
28d
56d
S T S T S T S T
120
60
50
40
30
Relative GLUT1 protein expression
1.25
1
0.75
0.5
0.25
0
*
*
*
*
Day 3
Day 10
Day 28
Day 56
Relative GLUT1 mRNA expression
1.5
1
0.5
0
Day 3
Day 10
Day 28
Day 56

Figure 2.7A

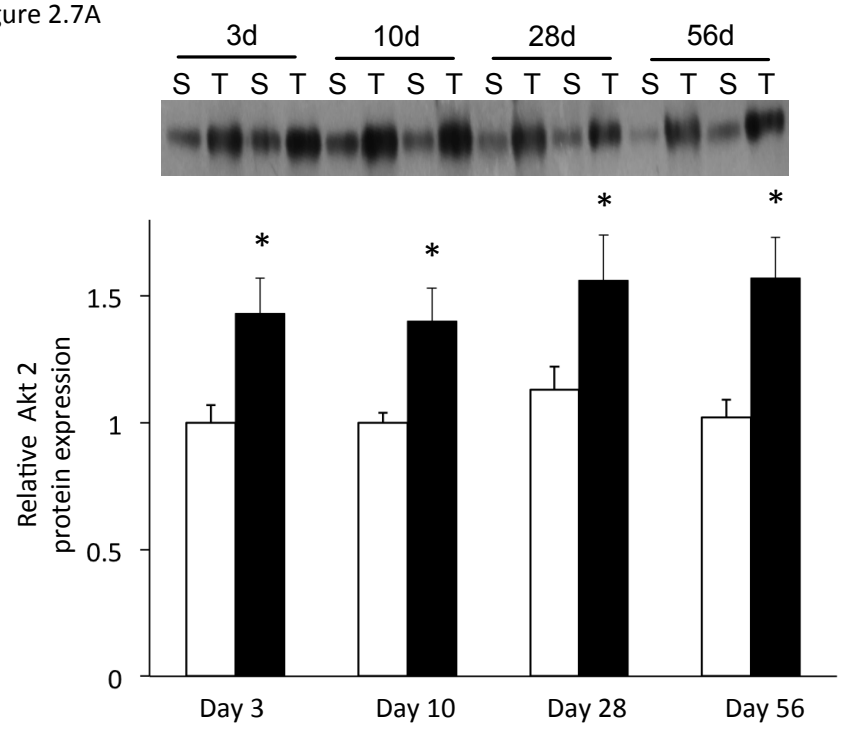
3d
10d
28d
56d
S T S T S T S T S T S T S T S T
Relative Akt 2 protein expression
1.5
1
0.5
0
*
*
*
*
Day 3
Day 10
Day 28
Day 56

Figure 2.7B

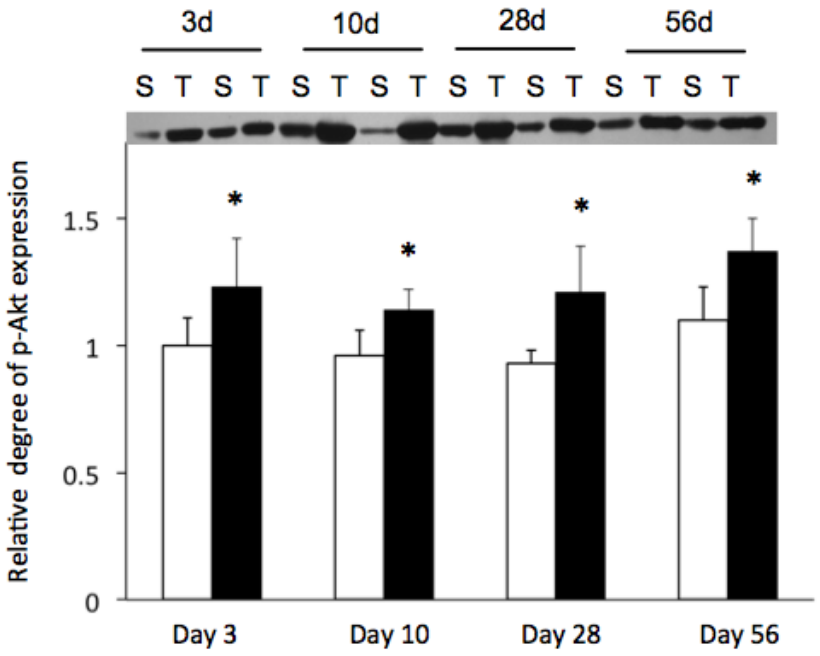
3d
10d
28d
56d
S T S T S T S T S T S T S T S T
Relative degree of p-Akt expression
1.5
1
0.5
0
*
*
*
*
Day 3
Day 10
Day 28
Day 56

CHAPTER 3

Prolonged high-fat feeding increases intramuscular triglycerides content and decreases glucose metabolism, but does not affect mitochondrial function

ABSTRACT

Incidence of diabetes is highly correlated with obesity; however, there is a lack of research elucidating the temporal progression into a diabetic phenotype. It has been proposed that increased lipid accumulation in non-adipose tissue may cause cellular death, including mitochondrial dysfunction, leading to the development of diabetes. Transgenic or non-transgenic FVB/N UCP-dta mice fed either a high-fat or normal-chow diet and were studied at 6, 9, 12, 15, 18, 21, and 24 weeks of age in order to identify temporal changes in body composition, IMTG content, glucose metabolism, and mitochondrial function under conditions of prolonged high-fat feeding in order to determine if IMTG drove mitochondrial dysfunction, leading to the development of diabetes. High-fat fed transgenic mice had a significantly greater body mass, lipid mass, and intramuscular triglyceride (IMTG) content. There was no difference in any of these measures for the other 3 groups. A glucose tolerance test revealed that high-fat fed transgenic mice had a significantly greater glucose area under the curve as compared to the other 3 groups. Plasma was collected every three weeks and transgenic high-fat fed mice demonstrated a significantly greater plasma insulin concentration. High-fat fed mice of both genotypes also had a significantly greater plasma non-esterified fatty acid and significantly lower plasma triglyceride content than normal-chow fed mice. There was no significant difference in either citrate synthase or cytochrome C oxidase enzyme activity in skeletal muscle among any groups. Additionally, there was no difference in expression of genes encoding transcriptional regulators of metabolism (PPARα, PPARδ, PGC-1α, PGC-1β), fatty acid metabolism (M-CPT I, CD36, MCAD) or mitochondrial oxidation (CS, CCO, ATP Synthase). It is possible that prolonged condition of elevated IMTG content and a developing diabetic condition will lead to mitochondrial defects. However, it does not appear that lipotoxicity is driving defects in mitochondrial function, which subsequently lead to a diabetic condition. Long-term high-fat feeding in transgenic mice produced increases in IMTG, adiposity, body mass, and plasma insulin accompanied by decreases in glucose metabolism, but did not reveal any deficits in mitochondrial function or regulation during the early stage of the development of type-2 diabetes.

Key Words: Intramuscular triglycerides, obesity, diabetes, glucose uptake

INTRODUCTION

The world is experiencing an epidemic of obesity and obesity-related metabolic disorders (collectively called metabolic syndrome), including cardiovascular disease, hypertension and diabetes. It is estimated that approximately 2.1 billion people (1/3 of the worldwide population) are overweight or obese (36) and that ~80% of type 2 diabetics are overweight or obese (1). There is a strong relationship between an increasing body mass index and prevalence of type 2 diabetes (2). In the United States, there are 25.8 million diabetics and ~79 million are pre-diabetic (2) with diabetes being the 6th leading cause of mortality. Recent epidemiological research indicates that 40% of the adult US population could develop diabetes, with that percentage as high as 50% in minority populations (26). The incidence of diabetes is also rapidly increasing worldwide and the World Health Organization estimates that there are 350 million diabetics worldwide (26), presenting a huge challenge to healthcare systems and biomedical research now and for years to come.

Obesity is accompanied by increases in both visceral and intracellular lipids. There is evidence for the deleterious effects of visceral lipid accumulation in numerous pathologies including congestive heart failure, ventricular abnormalities, hepatic fibrosis, and lipid-induced apoptosis (3, 30, 47). Visceral lipid accumulation is shown to reduce insulin-stimulated glucose metabolism and is also correlated with accumulation of increased intrahepatocellular lipids (IHCL) (8). Increases in IHCL may lead to non-alcoholic fatty liver disease, a condition that is associated with metabolic syndrome and insulin resistance (31). In addition to increases in IHCL, obesity is also often accompanied by an accumulation of lipids in cardiac muscle. The negative relationship between excessive intracellular lipids and cardiac myopathy was first described more than 40 years ago (6). In non-adipose tissues, changes in endoplasmic reticulum (ER) lipid composition may cause ER stress and mis-folding of proteins along with the initiation of the unfolded protein response (UPR) which slows protein translation and increases production of chaperone proteins (11, 29). If the UPR is unsuccessful, additional ER stress-related apoptosis mechanisms are initiated, inhibiting normal protein synthesis. There is also evidence of a strong negative association between pancreatic lipids and β-cell dysfunction (47, 54, 55), further exacerbating glucose metabolism. The

association between increased intracellular lipids and metabolic dysfunction led to a proposed theory of "lipotoxicity," in which increased intracellular lipid accumulation was not merely correlative, but was causative of insulin resistance and other metabolic disorders (55).

Like cardiac and pancreatic tissue, increases in intracellular triglycerides in skeletal muscle (IMTG) are correlated with deficits in glucose homeostasis (14, 49, 50). As skeletal muscle accounts for approximately 70% of whole-body glucose metabolism (48), decrements in the ability of skeletal muscle to maintain glucose homeostasis can have widespread effects in whole-body glucose metabolism. Numerous studies show a negative correlation between insulin sensitivity and IMTG (22, 24, 38, 40, 43). Recent studies have also shown that increased IMTG are associated with a preference towards lipid oxidation and a reduction in glucose metabolism (45, 52, 59). However, other investigations revealed a paradox to the "lipotoxicity" theory as endurance-trained athletes exhibit similarly high levels of intramuscular lipids as obese, diabetic patients without impairment of insulin-stimulated glucose uptake (9, 13, 42). Further investigation is required to determine whether increased intracellular lipids are causative or merely correlated with metabolic dysfunction. Greater understanding of the relationship between increased IMTG and glucose metabolism is vital and could have widespread impacts on large segments of the global population.

In addition to reduced insulin sensitivity, impairment of mitochondrial function in skeletal muscle is reported in diabetic patients (18, 32, 39) and animal models of type-2 diabetes (5, 56). Obese subjects also demonstrate an inability to transition between lipid and glucose metabolism and have a subsequent increase in lipid oxidation (13). Recent investigations note several possible drivers of mitochondrial dysfunction in response to lipid accumulation, including reduced functional capacity (43) and a reduction in mitochondrial biogenesis (18). However, increases in mitochondrial number are reported in insulin resistant rats fed a high-fat diet (16). So, although the correlation between mitochondrial dysfunction and increased intramuscular lipids is clear, the mechanisms by which these factors affect disease states are unresolved (51).

A majority of these studies are correlational in nature and describe changes later in a diabetic condition. The temporal effects that high-fat feeding has and the progressive

changes in IMTG content, glucose metabolism, and mitochondrial function that occur during the development of a diabetic phenotype are unclear. The current study was designed using a longitudinal model, which allows for temporal changes in IMTG levels to be contrasted against changes in muscle mitochondrial function. Our investigations focused on elucidating possible defects in lipid storage/catabolism and mitochondrial function throughout the initial stages of the pathogenesis of diabetes. Furthermore, it is uncertain whether lipid accumulation or mitochondrial dysfunction are symptoms or drivers of diabetes. The time-course nature of the study will also help determine whether mitochondrial dysfunction drives increases in IMTG or if increases in IMTG drive mitochondrial dysfunction. As such, this study will provide evidence for or against the "lipotoxicity" theory that increased lipids are causative of mitochondrial defects and metabolic dysfunction and/or diabetes. Our hypothesis is that lipid accumulation will precede mitochondrial dysfunction and will drive further perturbations in metabolism, leading to the development of diabetes.

MATERIALS AND METHODS

Animals and diet

FVB/N UCP-dta mice (TG) were obtained from the Jackson Laboratory (Bar Harbor, Maine). A breeding colony was established at the Miami University Animal Care Facility and non-transgenic littermates were used as controls (CT). All mice were housed under conditions of controlled temperature and humidity with a 12:12-h light:dark cycle and given water ad libitum. Upon weaning, mice were randomly selected and fed either standard chow (CH)-15% of calories from lipids or high-fat diet (HF)-41% of calories from lipids (Harlan Laboratories, Indianapolis, IN). This created 4 different genotype/diet groups: control chow (CTCH), control high-fat (CTHF), transgenic chow (TGCH), and transgenic high-fat (TGHF). At 6 weeks of age a subset of mice (8-10 per diet/phenotype group) was randomly chosen, and longitudinal measurements of body mass and body composition were taken and a glucose tolerance test was performed. A second subset of mice (8-10/per diet/phenotype group at each time point) was randomly selected for sequential analysis of intramuscular lipid content, plasma metabolites, gene expression, and citrate synthase/cytochrome C enzyme activity. The mice from subset 2 were assigned a sacrifice date of 6, 9, 12, 15, 18, 21, or 24 weeks of age and plasma and gastrocnemius muscle were collected for procedures described below.

All animal experiments and euthanasia protocols were conducted in accordance with the National Institutes of Health guidelines for humane treatment of laboratory animals and were reviewed and approved by the Institutional Animal Care and Use Committee of Miami University.

Body Mass and Composition

Starting at six weeks of age, mice from subset 1 (n=8-10/group) were weighed twice weekly to generate growth curves. Additionally, lean mass and fat mass were determined via quantitative nuclear magnetic resonance (NMR) using an EchoMRI^{TM}-500, (Echo Medical Systems, Houston, TX) at 6 weeks of age, and every three weeks thereafter (9, 12, 15, 18, 21, or 24 weeks).

Glucose tolerance testing

Using the same subset of animals as above, beginning at 6 weeks of age and every three weeks thereafter (9, 12, 15, 18, 21, or 24 weeks), a glucose tolerance test was performed (n=8-10). After an overnight fast, a blood sample was collected from the tail vein and glucose concentration was measured by the glucose oxidase method with a reflectance glucometer (One Touch II, LifeScan, Milpitas, CA). A 10% glucose solution (1 mg glucose/g body wt.) was administered by intraperitoneal injection and subsequent blood samples were obtained 30 min, 60 min and 120 min after injection. Glucose area under the curve (AUC) calculations were performed following Tai (1994) except baseline (minute 0) plasma glucose concentration was subtracted to eliminate the effect of intra-individual variations.

Intramuscular lipid content determination

Beginning at 6 weeks of age and every three weeks thereafter (9, 12, 15, 18, 21, or 24 weeks), mice from the second subset were sacrificed and tissues collected (n=8-10/group at each time point). Lipids were extracted from a piece of the gastrocnemius (GC) muscle using a modified Folch method as described earlier (10). The gastrocnemius piece was excised, weighed, snap frozen in liquid nitrogen, and minced in 40ml of 2:1 chloroform to methanol. After 24 hours @ 4°C, the sample was filtered, 60ml of 1:1 H_20 and chloroform were added and was left overnight to separate via gravity in a separatory funnel. The lower phase was drained and evaporated under nitrogen stream using a N-EVAP 111 (Organomation, Berlin, MA). The remaining dry extract was weighed and the lipid content (as a percentage of original tissue mass) was obtained.

Plasma Analysis

After sacrifice, blood was drawn from the inferior vena cava of mice (n= 8-10/group at each time point). Samples were frozen in liquid nitrogen and stored at −80°C. Plasma was sent to the Mouse Metabolic Phenotyping Core at the University of Cincinnati for determination of plasma free fatty acids and triglyceride concentrations as well as plasma insulin and glucose concentrations using standard protocols.

Quantitative RT-PCR

Using gastrocnemius tissues collected from mice in subset 2 (n= 8-10/group at each time point), quantitative RT-PCR was used to assess expression levels of transcripts for several genes. Primers were obtained from Integrated DNA Technologies (Coralville, IA). RNA was isolated from GC muscle using the TRIzol method (Life Technologies, Grand Island, NY) according to manufacturer's instructions. RNA quality was assessed spectrophotometrically and quantified by absorption spectrophotometry at 260 and 280 nm (NanoDrop 1000, NanoDrop-Fisher Thermo Scientific, Rockford, IL). cDNA was generated from 1 ug of total RNA for each gastrocnemius muscle using qScript™ cDNA Synthesis Kit (Quanta Biosciences, Gaithersburg, MD) according to the manufacturer's instructions. Relative quantitative RT-PCR was subsequently performed with a RotorGene 3000 (Qiagen, Valencia, CA) system using SYBR Green Master Mix (Applied Biosystems, Foster City, CA). For each gene, real-time PCR was performed in duplicate wells on cDNA generated from the reverse transcription of 10 ng of total RNA. Primer efficiencies were validated and verified for all genes and expression data were normalized to 36B4 (acidic ribosomal phosphoprotein P0), which did not change with treatment. Genes investigated and primer sequences were: PPARα (Peroxisome proliferator-activated receptor alpha); PPARβ (Peroxisome proliferator-activated receptor beta; PGC-1α (Peroxisome proliferator-activated receptor gamma coactivator-1alpha); PGC-1β (Peroxisome proliferator-activated receptor gamma coactivator-1beta); CD36 (Fatty Acid Translocase); MCAD (Medium-chain acyl-CoA dehydrogenase); M-CPT I (Muscle Carnitine palmitoyltransferase I); ATP synthase (F0F1 complex); and Cytochrome C oxidase (CCO).

Citrate synthase and Cytochrome c enzyme activity

Using gastrocnemius tissues collected from mice in subset 2 (n= 8-10/group at each time point), assays for citrate synthase (CS) and cytochrome c (CCO) activity were performed following the methods of Berner and Puckett (4). Citrate synthase activity was determined from the reduction of DTNB (5,5' dithiobis-2-nitrobenzoic acid) at 412 nm in assay medium containing 100 mM Tris-HCL (pH=8.0), 0.1mM DTNB, 0.15mM acetyl-Coa, 0.15 mM oxaloacetate (omitted for control). CCO activity was determined from the oxidation of reduced cytochrome c at 550 nm against a reference of 0.075 mM

cytochrome C oxidized with 0.33% potassium ferricyanide. The CCO assay medium contained 100 mM potassium phosphate (pH=7.5) and 0.075 mM reduced cytochrome c. Cytochrome c was reduced with sodium hydrosulfite, and excess sodium hydrosulfite was removed by bubbling with air for 30 min. All assays were performed in duplicate on a temperature-controlled spectrophotometer (PerkinElmer Lambda 35, Hebron, KY) at 37 °C. CS and CCO reactions were followed for 5 minutes. Enzyme activities were calculated from the slope of the linear portion of the reactions. Enzyme activity is expressed as units/gram of wet tissue, where 1 unit is equal to 1 μmol of product/min.

Statistical analysis

A univariate split-plot repeated measures analysis of variance (ANOVA) analysis was performed on the data for body mass and composition as well as plasma glucose concentration measurements using JMP statistical software (version 11.0.0) with genotype, diet, and time as factors. Data for the intramuscular lipid content, plasma metabolite analysis, gene expression, and citrate synthase/cytochrome c enzyme activity assay was analyzed using ANOVA with genotype, diet, and time as factors. Pairwise comparisons are reported in the running text of the results section. When significant differences were detected in parameters, pairwise comparisons were run using the Tukey HSD method. The level of significance was set at $p < 0.05$. Data are presented as means ± S.E.M. (n).

RESULTS

Body Mass and Composition

To describe changes in body composition, mice from subset 1 were weighed and had an MRI to measure lean and fat mass every three weeks. There was a significant interaction effect of diet and genotype on body mass and lipid mass as revealed by repeated-measures analysis of variance ($p < 0.05$). Pairwise comparison revealed that transgenic mice receiving high-fat chow had significantly greater mass than the mice in the other three groups at 6 weeks of age and throughout the study (Figure 3.1A; $p < 0.05$). By week 24, the TGHF mice were approximately 90% heavier than mice in the other three groups. Only the combination of transgenic mice eating high-fat feed elicited changes in body mass and composition, as there were no significant differences in the mice in the other three groups at any time point in the study. By 12 weeks of age, TGHF mice had significantly greater lean mass than the other groups (Figure 3.1B; $p < 0.05$). TGHF mice also had a significantly greater amount of fat mass than the other groups at all time points (Figure 3.1B; $p < 0.05$). Similar to the overall body mass, the difference in fat mass between TGHF and the other mice continued to increase, such that at 24 weeks the TGHF had approximately 110% greater fat mass than the other three groups.

Measurement of Intramuscular Lipid Content

We measured intramuscular lipid content to assess the effects that high-fat feeding and genotype feeding had on muscle lipid composition. Mice from subset 2 were sacrificed and IMTG content was determined via the Folch method (Folch, 1957). ANOVA revealed that diet and genotype each had significant effects on IMTG content (Figure 3.2; $p < 0.05$) such that high-fat chow fed mice and transgenic mice had higher levels of IMTG. Additionally, there was a significant interaction between diet and genotype as noted by the greater IMTG content in the TGHF mice (Figure 3.2; $p < 0.05$). Pairwise comparison revealed that IMTG content in TGHF was greater than the other groups starting at 9 weeks and continuing throughout the study (Figure 3.2; $p < 0.05$). There were no significant differences in IMTG content among the other three groups at any time point.

Plasma Metabolites

Plasma was taken from sacrificed animals in order to note temporal changes that high-fat feeding had on metabolites throughout the time course of the study. ANOVA revealed that diet had a significant effect on plasma triglycerides as both high-fat fed groups had lower plasma triglyceride levels than both normal-chow fed groups. There was also a significant effect of diet ($p < 0.05$) on NEFA concentration with both control and transgenic high-fat fed mice having higher levels than normal-chow fed control and transgenic mice (data not shown). A significant interaction between diet and age ($p < 0.05$) was also noted, as there was an increase in NEFA levels in older, high-fat fed mice (data not shown). There was no significant effect of age, genotype, or diet alone on plasma glucose concentrations.

Plasma Insulin and Glucose Tolerance Testing

In order to examine the effects of high-fat feeding and track the progression of a diabetic phenotype, beginning at 6 weeks and continuing throughout the time course of the study plasma was drawn from sacrificed animals and glucose tolerance tests were performed on mice from subset 1. Genotype had a significant effect on plasma insulin (Figure 3.3, $p < 0.05$), driven by the huge increases noted in TGHF plasma insulin levels. Although genotype had a significant effect on plasma insulin ($p < 0.05$), pairwise comparison revealed that TGHF plasma insulin was significantly higher than the other groups by 12 weeks of age and remained higher throughout the remainder of the study (Figure 3.3; $p < 0.05$). There was a significant interaction effect of diet and genotype on glucose area under the curve (AUC) calculated from glucose tolerance tests (Figure 3.4; $p < 0.05$). Pairwise comparison revealed that the AUC in TGHF mice was significantly greater than the other groups, at weeks 9, 12, 21 and 24 (Figure 3.4; $p < 0.05$). The AUC difference at 9 weeks (~39% greater in TGHF) was similar to the AUC difference at 24 weeks (~ 36% greater). There was no significant difference in AUC among the other three groups at any time point.

Metabolic Enzyme Activity

To determine if high-fat feeding and/or genotype had an effect on muscle

mitochondrial function during the development of diabetes, we measured activity of citrate synthase (CS) and cytochrome c oxidase (CCO). ANOVA revealed that the interaction between age and genotype was significant for CS activity, driven by the higher activity levels seen in older, high-fat fed transgenic mice (Figure 3.5A; $p < 0.05$). Pairwise comparison showed that CS activity in TGHF was significantly higher than the other groups at 24 weeks (Figure 3.5A; $p < 0.05$). There were no significant ANOVA effects or pairwise comparisons for CCO enzyme activity at any time point (Figure 3.5B).

Expression of Genes of Metabolism and Metabolic Regulation

To note the effects that high-fat feeding or genotype had on metabolic flexibility, including fatty acid transport and mitochondrial function, we investigated genes that are involved in regulation of metabolism and found that there was no significant effect of age, diet or genotype on gene expression for PPARα, PPARδ, PGC-1α, or PGC-1β (Figure 3.6; $p > 0.05$ in all cases). Similarly, there was also no significant effect of age, diet, or genotype for expression of genes involved in fatty acid transport: MCPT1 and CD36; fatty acid oxidation MCAD; or mitochondrial function: ATP Synthase, Cytochrome c oxidase, and CS (Figure 3.7; $p > 0.05$ in all cases).

DISCUSSION

To our knowledge, this is the first report describing the longitudinal effects of high-fat feeding on IMTG levels and mitochondrial function at the onset of the pathophysiology of diabetes. Although studies have noted a correlation between increased IMTG, decreased mitochondrial function and diabetic conditions, (14, 49, 50) the exact role that either factor has on the development of diabetes is unclear. It is also possible that mitochondrial deficits and lipid accumulation are the result of a diabetic condition. As skeletal muscle is responsible for a majority of glucose metabolism, perturbations in muscle lipid content or metabolic function that impact glucose uptake could have severe effects on whole-body glucose homeostasis. It has been reported that lipid oxidation is increased and glucose spared in type 2 diabetics, but, again, it is unknown how this metabolic shift is related to the development of diabetes (12, 57). It has been proposed that accumulation of lipids in non-adipose tissue is causative for the death of cells (47). The lipotoxic effects of increased ectopic lipids have been widely reported, but subsequent studies described a condition commonly known as the "athlete's paradox," in which the accumulation of IMTG in athletes is similar to that of obese, type II diabetics, but normal metabolic function is preserved (13). Although endurance training increases IMTG content, there have been no reports of increased lipid content in pancreatic or hepatic tissue. Therefore, this "athlete's paradox" suggests that it is not the mere presence of IMTG that is causative of metabolic dysfunction and demonstrate the clear need for research investigating the temporal relationship between metabolic substrate selection and mitochondrial stress (34), particularly in the pathogenesis of type 2 diabetes. Evidence supports an increased reliance on lipid oxidation and a lack of metabolic flexibility (17, 19, 21, 46, 52) as key factors in the development of diabetes.

The focus or our study was to describe the timeline of possible defects in lipid and carbohydrate metabolism and mitochondrial function throughout the development of a diabetic phenotype. Our results allow us to propose that increases in IMTG, increases in plasma insulin, and the failure to metabolize glucose efficiently precede defects in mitochondrial function and regulation. The UCP-dta mice express the diphtheria toxin A-chain under control of the uncoupling protein 1 promoter, which largely ablates brown adipose tissue (28), and when fed a "Western diet", develop marked obesity, insulin

resistance, hyperglycemia, and hyperlipidemia (15) and are often used as a murine model of diabetes. Consistent with previous findings, which described a large gain in body mass in mice fed a high-fat diet for 24 weeks (58), we noted a 66% difference in body mass of transgenic mice fed a high-fat diet for 18 weeks as compared to standard-chow fed transgenic or wild-type mice. Although our body composition data revealed that TGHF mice had a slightly higher lean mass than other groups, the TGHF mice had up to nearly 400% more fat mass than other groups. Prolonged high-fat feeding has been shown to increase IMTG content in other transgenic murine studies (7, 27) and our data confirm this with the TGHF mice having almost double the IMTG content of the other mice throughout the time course of the experiment.

The large difference in overall fat mass and IMTG content noted between TGHF and the other mice was not accompanied by increases in plasma triglycerides. There was an overall effect of diet in that both high-fat fed groups had slightly lower levels of plasma triglycerides and slightly higher plasma NEFA, which could be explained by an increased reliance on β-oxidation (16, 23, 36) and metabolic inflexibility (17, 36) reported previously in diabetic models. Although plasma triglycerides and NEFA levels were similar between both high-fat groups, plasma insulin levels in TGHF mice were ~ 500% greater. Further evidence to support the reliance upon lipid metabolism and metabolic inflexibility can be seen in the results of the glucose tolerance test, which showed that at 24 weeks the TGHF mice had a 36% larger area under the curve, indicating that the TGHF were starting to lose the ability to metabolize glucose effectively. Clearly, diet has an effect of altering blood chemistry, but only in the transgenic mice do we see the connection between increased plasma NEFA and increases visceral and intramuscular adiposity.

It has been reported previously that mice fed high-fat chow for two-weeks have decreased citric acid cycle function accompanied by increased β-oxidation and respiratory chain activity (44). We noted no changes in gene expression for CS, CCO, ATP Synthase, MCAD, CD36, or M-CPT I, so although IMTG content in TGHF mice was quite high, even in the early stages of the experiment, there was no evidence of any change in expression of genes involved in mitochondrial function, fatty acid metabolism or glycolysis at any time point. Thus, the high levels of IMTG and plasma insulin,

accompanied by decreased glucose uptake, without corresponding deficits in mitochondrial function indicate that mitochondrial dysfunction does not appear to drive insulin insensitivity or increases in IMTG. These data support previous findings which show that not only does high-fat feeding have little effect on mitochondrial function in rodents, there have been reports of upregulation of mitochondrial enzymes and mitochondrial transcriptional factors (16, 20, 37, 53). These results are also similar to those reported previously in human athletes, which saw no difference in insulin sensitivity in endurance trained individuals with high IMTG levels (13). As predicted, we also saw no evidence for a decrease in the expression of transcriptional regulators of mitochondrial function, as expression of PPARα, PPARβ, and PGC-1α and PGC-1β were unchanged throughout the pathogenesis of diabetes. Similarly, in humans it has been reported that insulin-resistant offspring of type 2 diabetic parents showed reduced mitochondrial density without changes in PGC-1α or PGC-1β (33). Therefore, it does not appear that mitochondrial dysfunction is a precursor of increased IMTG content or defects in glucose metabolism.

Although there is a strong correlation between obesity and diabetes, there is a lack of temporal studies describing the effects that increased IMTG has on mitochondrial function and insulin sensitivity of skeletal muscle during the development of a diabetic condition. In our study, we noted an early increase in body mass and lipid mass accompanied by significantly greater IMTG content. These differences were accompanied by a reduction in glucose metabolism and a significantly greater plasma insulin concentration. Neither the changes in body mass and composition, nor the deficit in glucose metabolism were accompanied by differences in mitochondrial function or transcriptional regulation of mitochondria. Our results help describe the temporal phenotypical changes in adiposity and glucose metabolism, that occur without significant decrements in mitochondrial function. This lends additional support to previous studies, which discounted lipotoxicity as the cause of mitochondrial dysfunction. The projected growth of the diabetes epidemic clearly requires continued investigation into the etiology of the disease to hopefully identify early biological markers for either lifestyle changes or pharmaceutical intervention.

REFERENCES

1. Astrup A, Finer N. Redefining type 2 diabetes: “diabesity” or “obesity dependent diabetes mellitus”? *Obes Rev* 1: 57–59, 2000.

2. Bays HE, Bazata DD, Clark NG, Gavin JR, Green AJ, Lewis SJ, Reed ML, Stewart W, Chapman RH, Fox KM, Grandy S. Prevalence of self-reported diagnosis of diabetes mellitus and associated risk factors in a national survey in the US population: SHIELD (Study to Help Improve Early evaluation and management of risk factors Leading to Diabetes). *BMC Public Health* 7: 277, 2007.

3. Berkalp B, Cesur V, Corapcioglu D, Erol C, Baskal N. Obesity and left ventricular diastolic dysfunction. *Int J Cardiol* 52: 23–6, 1995.

4. Berner NJ, Puckett RE. Phenotypic flexibility and thermoregulatory behavior in the eastern red-spotted newt (Notophthalmus viridescens viridescens). *J Exp Zool Part A Ecol Genet Physiol* 313 A: 231–239, 2010.

5. Boudina S, Sena S, O’Neill BT, Tathireddy P, Young ME, Abel ED. Reduced mitochondrial oxidative capacity and increased mitochondrial uncoupling impair myocardial energetics in obesity. *Circulation* 112: 2686–2695, 2005.

6. Chu KC, Sohal RS, Sun SC, Burch GE, Colcolough HL. Lipid cardiomyopathy of the hypertrophied heart of goldthioglucose obese mice. *J Pathol* 97: 99–103, 1969.

7. Costford SR, Chaudhry SN, Salkhordeh M, Harper M-E. Effects of the presence, absence, and overexpression of uncoupling protein-3 on adiposity and fuel metabolism in congenic mice. *Am J Physiol Endocrinol Metab* 290: E1304–12, 2006.

8. Deivanayagam S, Mohammed BS, Vitola BE, Naguib GH, Keshen TH, Kirk EP, Klein S. Nonalcoholic fatty liver disease is associated with hepatic and skeletal muscle insulin resistance in overweight adolescents. *Am J Clin Nutr* 88: 257–62, 2008.

9. Dubé JJ, Amati F, Stefanovic-Racic M, Toledo FGS, Sauers SE, Goodpaster BH. Exercise-induced alterations in intramyocellular lipids and insulin resistance: the athlete’s paradox revisited. *Am J Physiol Endocrinol Metab* 294: E882–E888, 2008.

10. Folch J, Lees M, Sloane GH. A simple method for the isolation and purification of total lipides from animal tissues. *J Biol Chem* 226: 497–509, 1957.

11. Fu S, Yang L, Li P, Hofmann O, Dicker L, Hide W, Lin X, Watkins SM, Ivanov AR, Hotamisligil GS. Aberrant lipid metabolism disrupts calcium homeostasis causing liver endoplasmic reticulum stress in obesity. *Nature* 473: 528–31, 2011.

12. Galgani J, Ravussin E. Energy metabolism, fuel selection and body weight regulation. *Int J Obes (Lond)* 32 Suppl 7: S109–S119, 2008.

13. Goodpaster BH, He J, Watkins S, Kelley DE. Skeletal muscle lipid content and insulin resistance: Evidence for a paradox in endurance-trained athletes. *J Clin Endocrinol Metab* 86: 5755–5761, 2001.

14. Goodpaster BH, Thaete FL, Simoneau JA, Kelley DE. Subcutaneous abdominal fat and thigh muscle composition predict insulin sensitivity independently of visceral fat. *Diabetes* 46: 1579–85, 1997.

15. Hamann A, Flier JS, Lowell BB. Decreased brown fat markedly enhances susceptibility to diet-induced obesity, diabetes, and hyperlipidemia. *Endocrinology* 137: 21–9, 1996.

16. Hancock CR, Han D-H, Chen M, Terada S, Yasuda T, Wright DC, Holloszy JO. High-fat diets cause insulin resistance despite an increase in muscle mitochondria. *Proc Natl Acad Sci U S A* 105: 7815–7820, 2008.

17. Van Herpen NA, Schrauwen-Hinderling VB, Schaart G, Mensink RP, Schrauwen P. Three weeks on a high-fat diet increases intrahepatic lipid accumulation and decreases metabolic flexibility in healthy overweight men. *J Clin Endocrinol Metab* 96: E691–5, 2011.

18. Kelley DE, He J, Menshikova E V., Ritov VB. Dysfunction of Mitochondria in Human Skeletal Muscle in Type 2 Diabetes . *Diabetes* 51: 2944–2950, 2002.

19. Kelley DE, Mandarino LJ. Fuel selection in human skeletal muscle in insulin resistance: a reexamination. *Diabetes* 49: 677–83, 2000.

20. Koves TR, Li P, An J, Akimoto T, Slentz D, Ilkayeva O, Dohm GL, Yan Z, Newgard CB, Muoio DM. Peroxisome proliferator-activated receptor-gamma co-activator 1alpha-mediated metabolic remodeling of skeletal myocytes mimics exercise training and reverses lipid-induced mitochondrial inefficiency. *J Biol Chem* 280: 33588–98, 2005.

21. Koves TR, Ussher JR, Noland RC, Slentz D, Mosedale M, Ilkayeva O, Bain J, Stevens R, Dyck JRB, Newgard CB, Lopaschuk GD, Muoio DM. Mitochondrial overload and incomplete fatty acid oxidation contribute to skeletal muscle insulin resistance. *Cell Metab* 7: 45–56, 2008.

22. Kraegen EW, Clark PW, Jenkins AB, Daley EA, Chisholm DJ, Storlien LH. Development of muscle insulin resistance after liver insulin resistance in high-fat-fed rats. *Diabetes* 40: 1397–403, 1991.

23. Kraegen EW, Cooney GJ, Turner N. Muscle insulin resistance: a case of fat overconsumption, not mitochondrial dysfunction. *Proc Natl Acad Sci U S A* 105: 7627–8, 2008.

24. Krssak M, Falk Petersen K, Dresner A, DiPietro L, Vogel SM, Rothman DL, Roden M, Shulman GI. Intramyocellular lipid concentrations are correlated with insulin sensitivity in humans: a 1H NMR spectroscopy study. *Diabetologia* 42: 113–6, 1999.

25. Lam DW, LeRoith D. The worldwide diabetes epidemic. *Curr Opin Endocrinol Diabetes Obes* 19: 93–6, 2012.

26. Lipscombe LL. The US diabetes epidemic: tip of the iceberg. *Lancet Diabetes Endocrinol.* 2: 854-855 2014.

27. Liu L, Zhang Y, Chen N, Shi X, Tsang B, Yu Y-H. Upregulation of myocellular DGAT1 augments triglyceride synthesis in skeletal muscle and protects against fat-induced insulin resistance. *J Clin Invest* 117: 1679–89, 2007.

28. Lowell BB, S-Susulic V, Hamann A, Lawitts JA, Himms-Hagen J, Boyer BB, Kozak LP, Flier JS. Development of obesity in transgenic mice after genetic ablation of brown adipose tissue. *Nature* 366: 740–2, 1993.

29. Malhotra JD, Kaufman RJ. The endoplasmic reticulum and the unfolded protein response. *Semin Cell Dev Biol* 18: 716–731, 2007.

30. Marceau P, Biron S, Hould FS, Marceau S, Simard S, Thung SN, Kral JG. Liver pathology and the metabolic syndrome X in severe obesity. *J Clin Endocrinol Metab* 84: 1513–7, 1999.

31. Marchesini G, Brizi M, Bianchi G, Tomassetti S, Bugianesi E, Lenzi M, McCullough AJ, Natale S, Forlani G, Melchionda N. Nonalcoholic fatty liver disease: a feature of the metabolic syndrome. *Diabetes* 50: 1844–50, 2001.

32. Mootha VK, Lindgren CM, Eriksson K-F, Subramanian A, Sihag S, Lehar J, Puigserver P, Carlsson E, Ridderstråle M, Laurila E, Houstis N, Daly MJ, Patterson N, Mesirov JP, Golub TR, Tamayo P, Spiegelman B, Lander ES, Hirschhorn JN, Altshuler D, Groop LC. PGC-1alpha-responsive genes involved in oxidative phosphorylation are coordinately downregulated in human diabetes. *Nat Genet* 34: 267–273, 2003.

33. Morino K, Petersen KF, Dufour S, Befroy D, Frattini J, Shatzkes N, Neschen S, White MF, Bilz S, Sono S, Pypaert M, Shulman GI. Reduced mitochondrial density and increased IRS-1 serine phosphorylation in muscle of insulin-resistant offspring of type 2 diabetic parents. *J Clin Invest* 115: 3587–93, 2005.

34. Muoio DM. Intramuscular triacylglycerol and insulin resistance: guilty as charged or wrongly accused? *Biochim Biophys Acta* 1801: 281–8, 2010.

35. Ng M, Fleming T, Robinson M, Thomson B, Graetz N, Margono C, Mullany EC, Biryukov S, Abbafati C, Abera SF, Abraham JP, Abu-Rmeileh NM, Achoki T, AlBuhairan FS, Alemu ZA, Alfonso R, Ali MK, Ali R, Guzman NA, Ammar W, Anwari P, Banerjee A, Barquera S, Basu S, Bennett DA, Bhutta Z, Blore J, Cabral N, Nonato IC, Chang JC, Chowdhury R, Courville KJ, Criqui MH, Cundiff DK, Dabhadkar KC, Dandona L, Davis A, Dayama A, Dharmaratne SD, Ding EL, Durrani AM, Esteghamati A, Farzadfar F, Fay DF, Feigin VL, Flaxman A, Forouzanfar MH, Goto A, Green MA, Gupta R, Hafezi-Nejad N, Hankey GJ, Harewood HC, Havmoeller R, Hay S, Hernandez L, Husseini A, Idrisov BT, Ikeda N, Islami F, Jahangir E, Jassal SK, Jee SH, Jeffreys M, Jonas JB, Kabagambe EK, Khalifa SE, Kengne AP, Khader YS, Khang YH, Kim D, Kimokoti RW, Kinge JM, Kokubo Y, Kosen S, Kwan G, Lai T, Leinsalu M, Li Y, Liang X, Liu S, Logroscino G, Lotufo PA, Lu Y, Ma J, Mainoo NK, Mensah GA, Merriman TR, Mokdad AH, Moschandreas J, Naghavi M, Naheed A, Nand D, Narayan KM, Nelson EL, Neuhouser ML, Nisar MI, Ohkubo T, Oti SO, Pedroza A, Prabhakaran D, Roy N, Sampson U, Seo H, Sepanlou SG, Shibuya K, Shiri R, Shiue I, Singh GM, Singh JA, Skirbekk V, Stapelberg NJ, Sturua L, Sykes BL, Tobias M, Tran BX, Trasande L, Toyoshima H, van de Vijver S, Vasankari TJ, Veerman JL, Velasquez-Melendez G, Vlassov V V, Vollset SE, Vos T, Wang C, Wang SX, Weiderpass E, Werdecker A, Wright JL, Yang YC, Yatsuya H, Yoon J, Yoon SJ, Zhao Y, Zhou M, Zhu S, Lopez AD, Murray CJ, Gakidou E. Global, regional, and national prevalence of overweight and obesity in children and adults during 1980-2013: a systematic analysis for the Global Burden of Disease Study 2013. *Lancet* 2014.

36. Noland RC, Koves TR, Seiler SE, Lum H, Lust RM, Ilkayeva O, Stevens RD, Hegardt FG, Muoio DM. Carnitine insufficiency caused by aging and overnutrition compromises mitochondrial performance and metabolic control. *J Biol Chem* 284: 22840–52, 2009.

37. Noland RC, Woodlief TL, Whitfield BR, Manning SM, Evans JR, Dudek RW, Lust RM, Cortright RN. Peroxisomal-mitochondrial oxidation in a rodent model of obesity-associated insulin resistance. *Am J Physiol Endocrinol Metab* 293: E986–E1001, 2007.

38. Pan DA, Lillioja S, Kriketos AD, Milner MR, Baur LA, Bogardus C, Jenkins AB, Storlien LH. Skeletal muscle triglyceride levels are inversely related to insulin action. *Diabetes* 46: 983–8, 1997.

39. Patti ME, Butte AJ, Crunkhorn S, Cusi K, Berria R, Kashyap S, Miyazaki Y, Kohane I, Costello M, Saccone R, Landaker EJ, Goldfine AB, Mun E, DeFronzo R, Finlayson J, Kahn CR, Mandarino LJ. Coordinated reduction of genes of oxidative metabolism in humans with insulin resistance and diabetes: Potential role of PGC1 and NRF1. *Proc Natl Acad Sci U S A* 100: 8466–8471, 2003.

40. Phillips DI, Caddy S, Ilic V, Fielding BA, Frayn KN, Borthwick AC, Taylor R. Intramuscular triglyceride and muscle insulin sensitivity: evidence for a relationship in nondiabetic subjects. *Metabolism* 45: 947–50, 1996.

41. Ritov VB, Menshikova E V., He J, Ferrell RE, Goodpaster BH, Kelley DE. Deficiency of subsarcolemmal mitochondria in obesity and type 2 diabetes. *Diabetes* 54: 8–14, 2005.

42. Russell AP. Lipotoxicity: the obese and endurance-trained paradox. *Int J Obes Relat Metab Disord* 28 Suppl 4: S66–S71, 2004.

43. Russell JC, Shillabeer G, Bar-Tana J, Lau DC, Richardson M, Wenzel LM, Graham SE, Dolphin PJ. Development of insulin resistance in the JCR:LA-cp rat: role of triacylglycerols and effects of MEDICA 16. *Diabetes* 47: 770–8, 1998.

44. Sadler NC, Angel TE, Lewis MP, Pederson LM, Chauvigné-Hines LM, Wiedner SD, Zink EM, Smith RD, Wright AT. Activity-based protein profiling reveals mitochondrial oxidative enzyme impairment and restoration in diet-induced obese mice. *PLoS One* 7: e47996, 2012.

45. Sapiro JM, Mashek MT, Greenberg AS, Mashek DG. Hepatic triacylglycerol hydrolysis regulates peroxisome proliferator-activated receptor alpha activity. *J Lipid Res* 50: 1621–1629, 2009.

46. Seiler SE, Martin OJ, Noland RC, Slentz DH, DeBalsi KL, Ilkayeva OR, An J, Newgard CB, Koves TR, Muoio DM. Obesity and lipid stress inhibit carnitine acetyltransferase activity. *J Lipid Res* 55: 635–44, 2014.

47. Shimabukuro M, Zhou YT, Levi M, Unger RH. Fatty acid-induced beta cell apoptosis: a link between obesity and diabetes. *Proc Natl Acad Sci USA* 95: 2498–502, 1998.

48. Shulman GI, Rothman DL, Jue T, Stein P, DeFronzo RA, Shulman RG. Quantitation of muscle glycogen synthesis in normal subjects and subjects with non-insulin-dependent diabetes by 13C nuclear magnetic resonance spectroscopy. *N Engl J Med* 322: 223–8, 1990.

49. Simoneau JA, Colberg SR, Thaete FL, Kelley DE. Skeletal muscle glycolytic and oxidative enzyme capacities are determinants of insulin sensitivity and muscle composition in obese women. *FASEB J* 9: 273–8, 1995.

50. Simoneau JA, Kelley DE. Altered glycolytic and oxidative capacities of skeletal muscle contribute to insulin resistance in NIDDM. *J Appl Physiol* 83: 166–71, 1997.

51. Storlien L, Oakes ND, Kelley DE. Metabolic flexibility. *Proc Nutr Soc* 63: 363–368, 2004.

52. Thyfault JP, Rector RS, Noland RC. Metabolic inflexibility in skeletal muscle: a prelude to the cardiometabolic syndrome? *J Cardiometab Syndr* 1: 184–9, 2006.

53. Turner N, Bruce CR, Beale SM, Hoehn KL, So T, Rolph MS, Cooney GJ. Excess lipid availability increases mitochondrial fatty acid oxidative capacity in muscle: evidence against a role for reduced fatty acid oxidation in lipid-induced insulin resistance in rodents. *Diabetes* 56: 2085–92, 2007.

54. Tushuizen ME, Bunck MC, Pouwels PJ, Bontemps S, van Waesberghe JHT, Schindhelm RK, Mari A, Heine RJ, Diamant M. Pancreatic fat content and beta-cell function in men with and without type 2 diabetes. *Diabetes Care* 30: 2916–21, 2007.

55. Unger RH. Lipotoxicity in the pathogenesis of obesity-dependent NIDDM: Genetic and clinical implications. *Diabetes* 44: 863–870, 1995.

56. Warren BE, Lou P-H, Lucchinetti E, Zhang L, Clanachan AS, Affolter A, Hersberger M, Zaugg M, Lemieux H. Early mitochondrial dysfunction in glycolytic muscle, but not oxidative muscle, of the fructose-fed insulin-resistant rat. *Am J Physiol Endocrinol Metab* 306: E658–67, 2014.

57. Van de Weijer T, Sparks LM, Phielix E, Meex RC, van Herpen NA, Hesselink MKC, Schrauwen P, Schrauwen-Hinderling VB. Relationships between Mitochondrial Function and Metabolic Flexibility in Type 2 Diabetes Mellitus. *PLoS One* 8, 2013.

58. Weisberg SP, Hunter D, Huber R, Lemieux J, Slaymaker S, Vaddi K, Charo I, Leibel RL, Ferrante AW. CCR2 modulates inflammatory and metabolic effects of high-fat feeding. *J Clin Invest* 116: 115–24, 2006.

59. Zechner R, Kienesberger PC, Haemmerle G, Zimmermann R, Lass A. Adipose triglyceride lipase and the lipolytic catabolism of cellular fat stores. *J Lipid Res* 50: 3–21, 2009.

TABLES

Table 3.1 Primer sequences for qPCR

Gene	Forward	Reverse
PPARα	ACTACGGAGTTCACGCATGTG	TTGTCGTCAACCAGCTTCAGC
PPARδ	TCACCGGCAAGTCCAGCC	ACACCAGGCCCTTCTCTGGCT
PGC-1α	CGGAAATCATATCCAACCAG	TGAGGACCACTAGCAAGTTTG
PGC1β	TCCAGAAGTCAGCGGCCT	CTGAGCCCGCAGTGTGG
MCAD	GGCTCCTGAGAAGTGTTTCTC	GGCTCCTGGTTGTGAGC
MCPT1	TCTAGGGAATGCCGTTCAC	GAGCACATGGGCACCATAC
CD36	CAAGCTCCTTGGCATGGTAGA	TGGATTTGCAAGCACAATATG
F0F1-ATPase	CGTGAGGGCAATGATTTATAC	TCCTGGTCTCTGAAGTATTCAG
CCO	ACCAAATCTCCACGGTCTGTT	GGATTCTCCAAATACTCCATC
CS	CAAGCAACATGGGAAGA	GTCAGGAAGAACCGAAGTCT
36B4	AGATGCAGCAGATCCGCAT	ATATGAGGCAGCAGTTTCTCC

FIGURE LEGENDS

Figure 3.1 High-fat chow leads to increases in body mass in transgenic mice. Mice were weighed twice weekly and lean/fat tissue mass was determined via NMR every three weeks. A. Overall body mass. B. Lean tissue mass (top), fat mass (bottom). (n = 8-10/group). Dashed lines represent chow fed mice, while solid lines represent high-fat fed mice. Squares represent control mice, while circles represent transgenic mice. Values are means ± SEM. Superscripted letter indicates significant interaction effect between diet and genotype (ANOVA; $p < 0.05$). * indicates significant pairwise differences between TGHF and the other groups ($p < 0.05$).

Figure 3.2 Transgenic mice fed high-fat chow have higher intramuscular lipid content. Intramuscular lipid content of the gastrocnemius muscle was measured via the Folch method. Values are means ± SEM, (n = 8-10). Superscripted letter indicates significant interaction effect between diet and genotype (ANOVA; $p < 0.05$). * indicates significant pairwise differences between TGHF and the other groups ($p < 0.05$).

Figure 3.3 Plasma insulin concentration is higher in transgenic mice fed high-fat chow. Blood was drawn from the inferior vena cava following sacrifice and plasma insulin concentration was measured. Values are means ± SEM, (n = 8-10). Superscripted letter indicates significant interaction effect between diet and genotype (ANOVA; $p < 0.05$). * indicates significant pairwise differences between TGHF and the other groups ($p < 0.05$). There are no error bars for TGHF mice at 21 and 24 weeks because all samples equaled or exceeded the maximum assay value of 110 ng/mL.

Figure 3.4 Glucose area under the curve is higher in TGHF mice. Glucose tolerance tests were performed every three weeks and calculations of glucose area under the curve were determined. Baseline (minute 0) plasma glucose levels were subtracted for each animal to eliminate inter-animal variability. Values are means ± SEM, (n = 8-10). Superscripted letter indicates significant interaction effect between diet and genotype (ANOVA; $p < 0.05$). * indicates significant pairwise differences between TGHF and the other groups ($p < 0.05$).

Figure 3.5 Citrate synthase activity is higher at 24 weeks in TGHF fed mice compared to TGCH mice, but cytochrome c oxidase activity is unchanged at any time point in homogenates of gastrocnemius muscle. A. CS enzyme activity B. CCO enzyme activity. Values are means ± SEM, (n = 8-10). # indicates significant pairwise differences between TGHF and TGCH ($p < 0.05$).

Figure 3.6 mRNA expression is not statistically different for genes involved in metabolic regulation in all groups throughout the time course of the study. A. PPARα B. PPARδ; C. PGC-1α D. PGC-1β. Quantitative data for each gene were normalized and corrected for the expression of a housekeeping gene (36B4). Values are means ± SEM, (n = 8-10).

Figure 3.7 mRNA expression is not statistically different for genes involved in fatty acid transport and mitochondrial function in all groups throughout the time course of the study. A. MCAD; B. M CPT-I; C. CD36; D. CS; E. ATP synthase; F. CCO oxidase. Quantitative data for each gene were normalized and corrected for the expression of a housekeeping gene (36B4). Values are means ± SEM, (n = 8-10).

FIGURES

Figure 3.1A

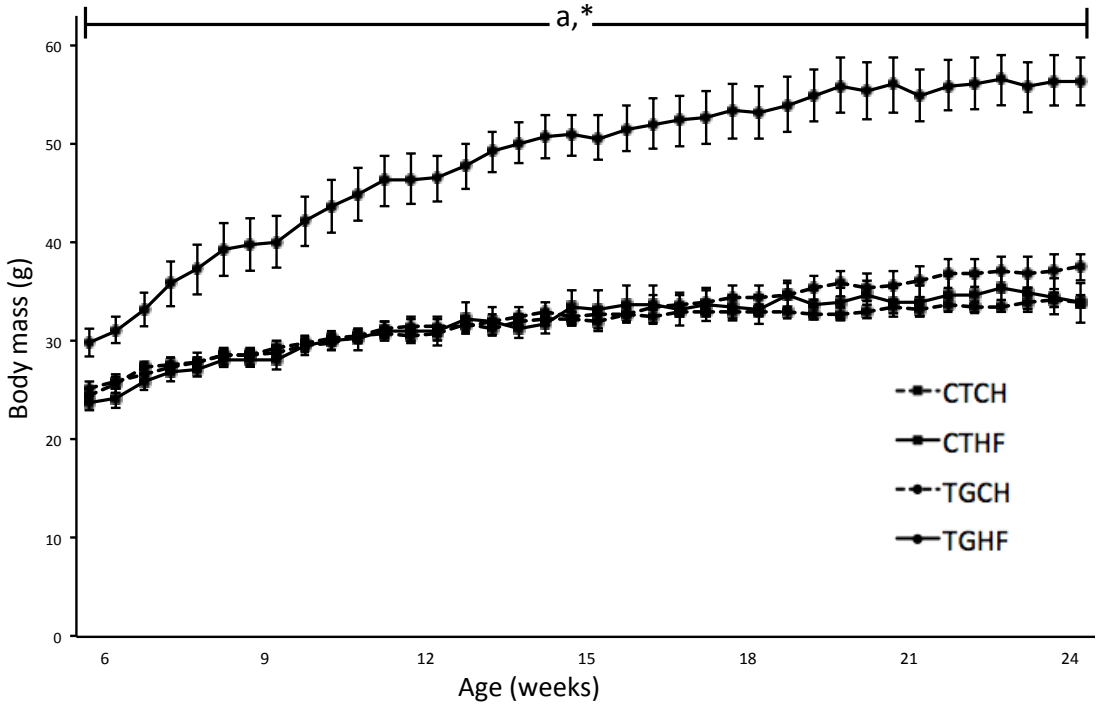

Figure 3.1B

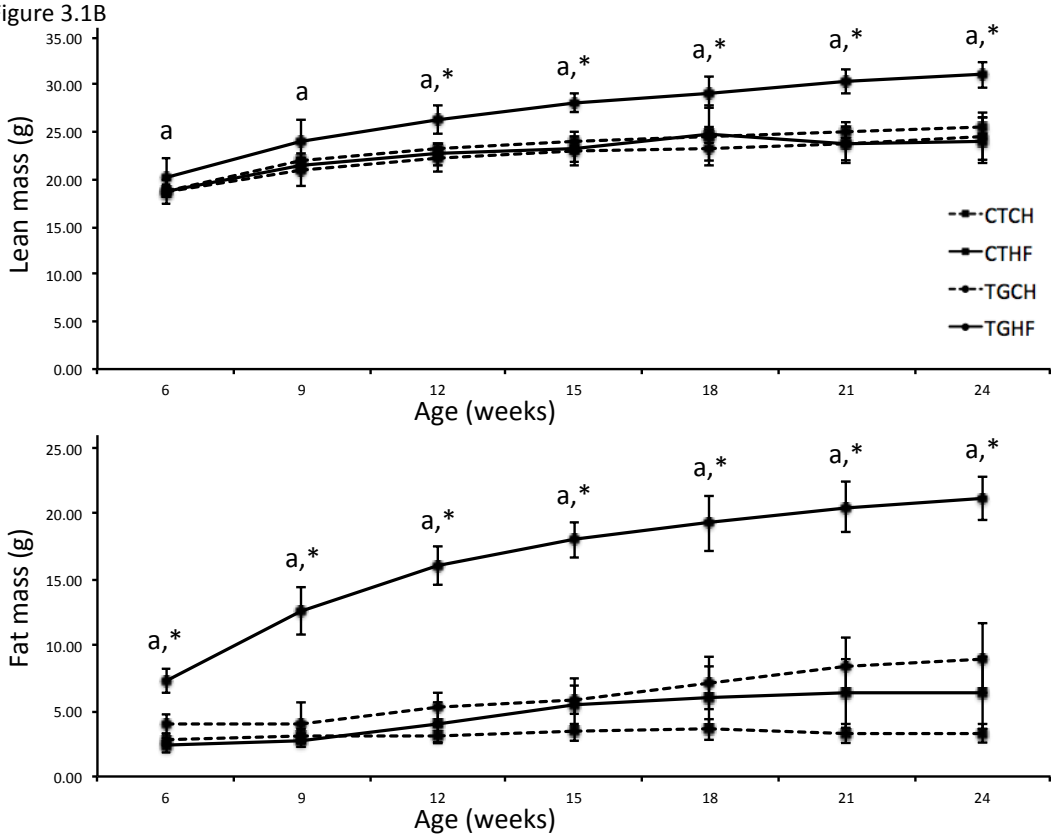
Lean mass (g)
35.00
30.00
25.00
20.00
15.00
10.00
5.00
0.00
a
a
a,*
a,*
a,*
a,*
a,*
6
9
12
15
18
21
24
Age (weeks)
CTCH
CTHF
TGCH
TGHF
Fat mass (g)
25.00
20.00
15.00
10.00
5.00
0.00
a,*
a,*
a,*
a,*
a,*
a,*
a,*
6
9
12
15
18
21
24
Age (weeks)

Figure 3.2.

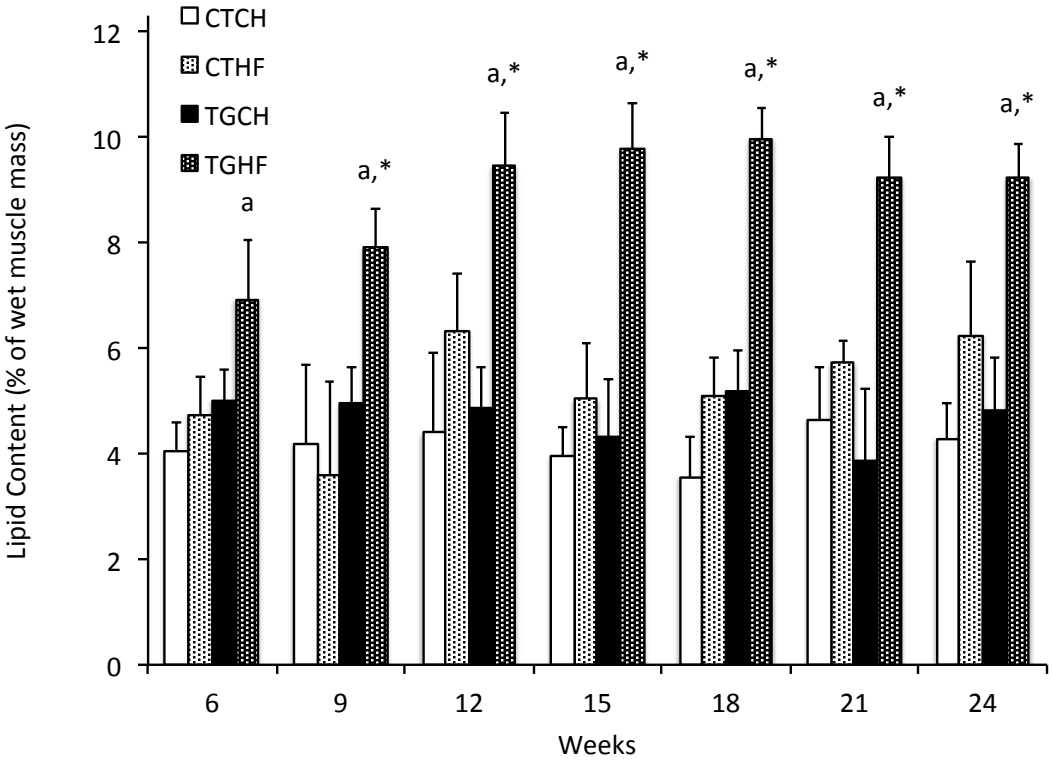
CTCH
CTHF
TGCH
TGHF
Lipid Content (% of wet muscle mass)
Weeks
0
2
4
6
8
10
12
6
9
12
15
18
21
24
a
a,*
a,*
a,*
a,*
a,*

Figure 3.3

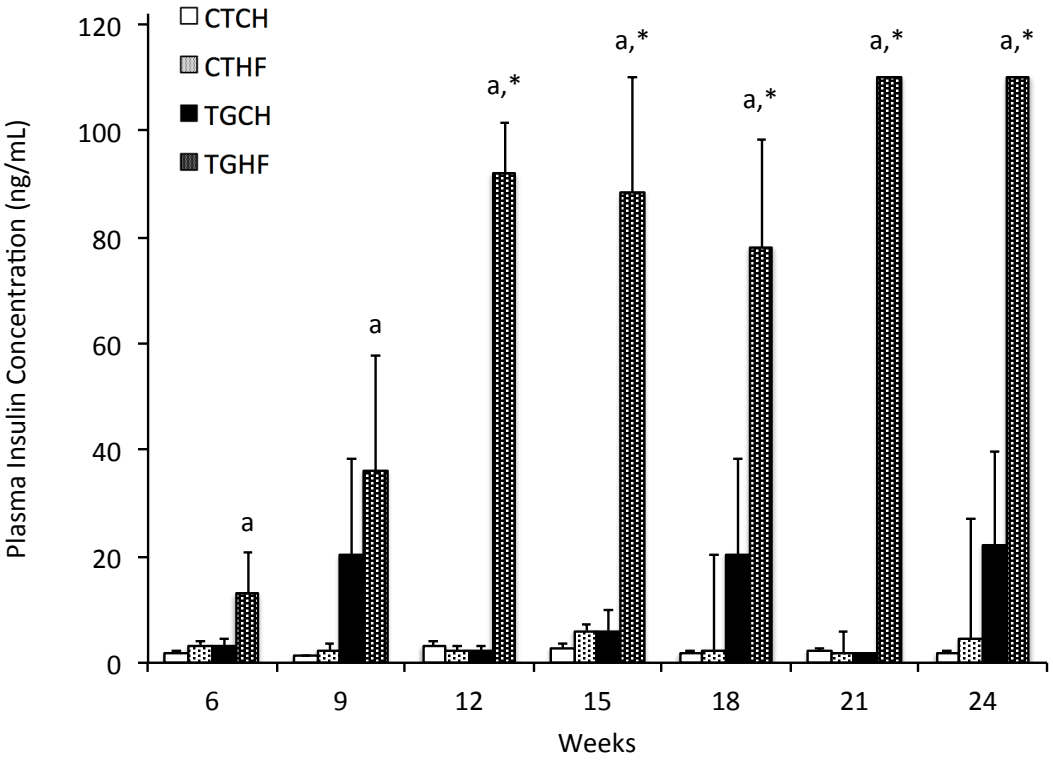
CTCH
CTHF
TGCH
TGHF
Plasma Insulin Concentration (ng/mL)
120
100
80
60
40
20
0
a
a
a,*
a,*
a,*
a,*
a,*
6
9
12
15
18
21
24
Weeks

Figure 3.4

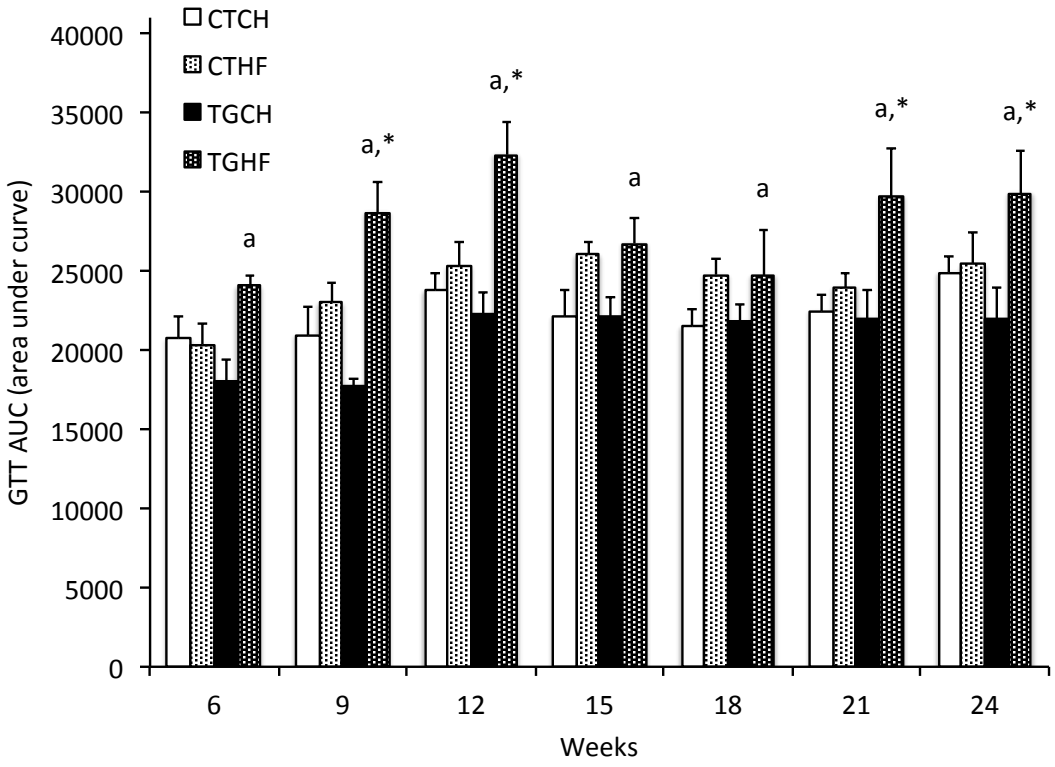
CTCH
CTHF
TGCH
TGHF
GTT AUC (area under curve)
40000
35000
30000
25000
20000
15000
10000
5000
0
a
a,*
a,*
a
a
a,*
a,*
6
9
12
15
18
21
24
Weeks

Figure 3.5A

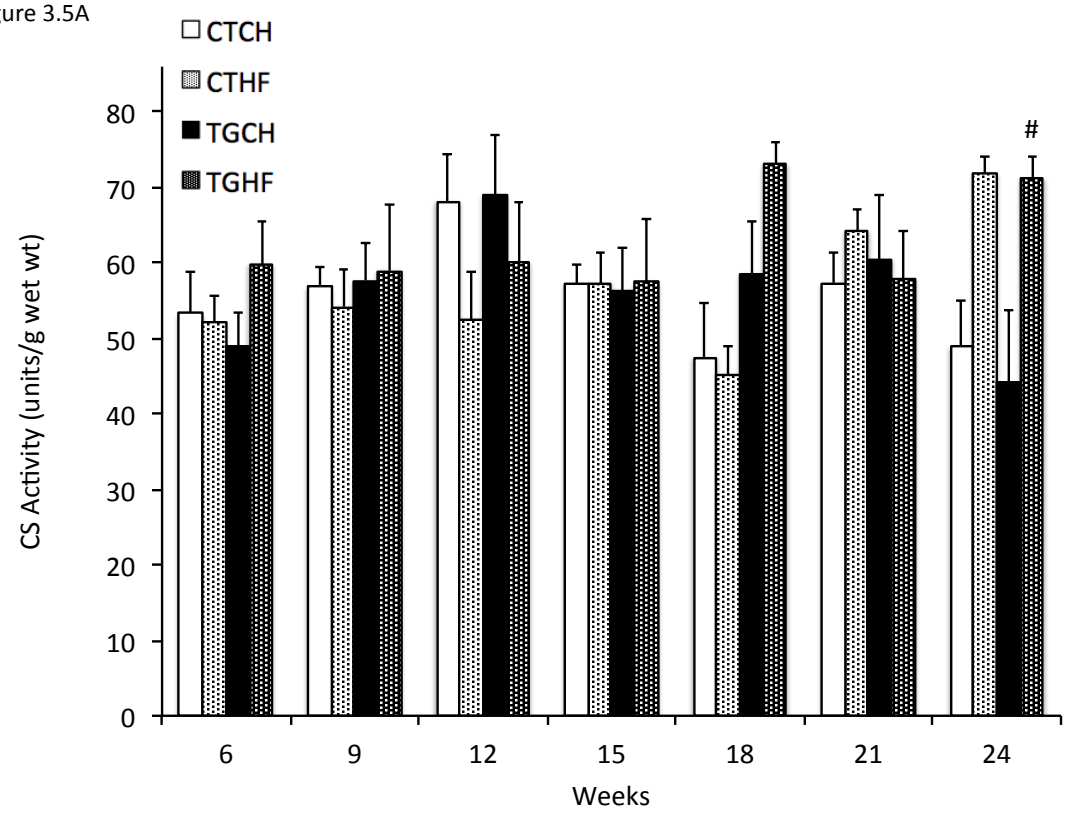
CTCH
CTHF
TGCH
TGHF
CS Activity (units/g wet wt)
0
10
20
30
40
50
60
70
80
#
6
9
12
15
18
21
24
Weeks

Figure 3.5B

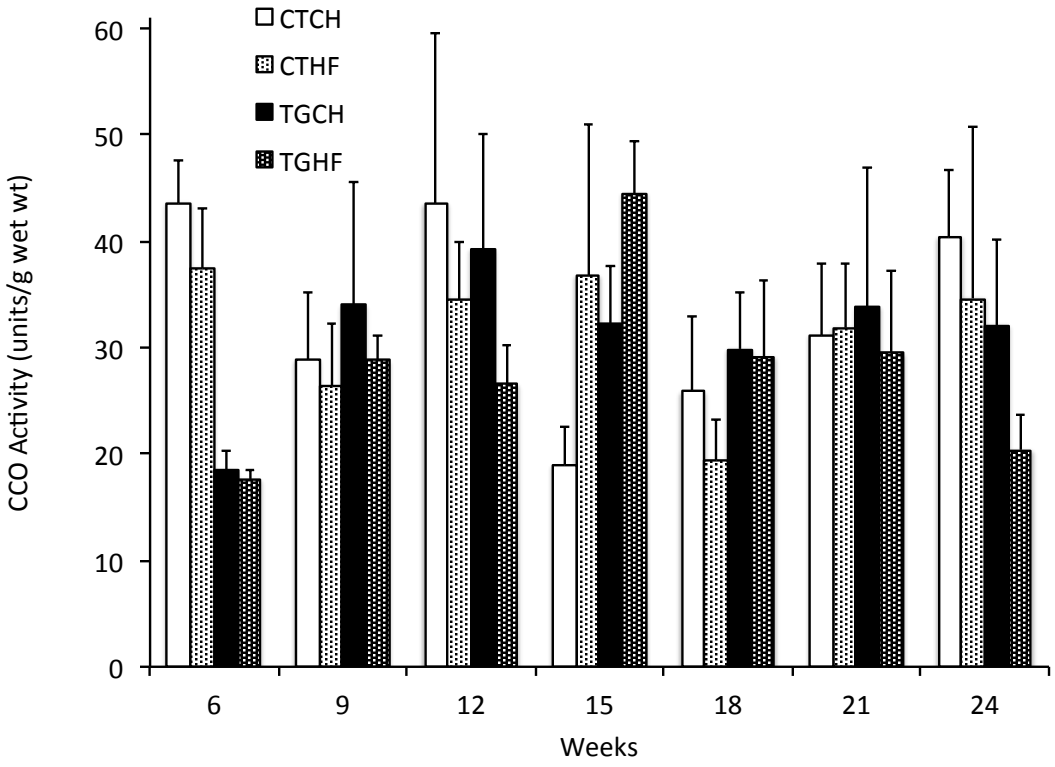
CTCH
CTHF
TGCH
TGHF
CCO Activity (units/g wet wt)
60
50
40
30
20
10
0
6
9
12
15
18
21
24
Weeks

Figure 3.6

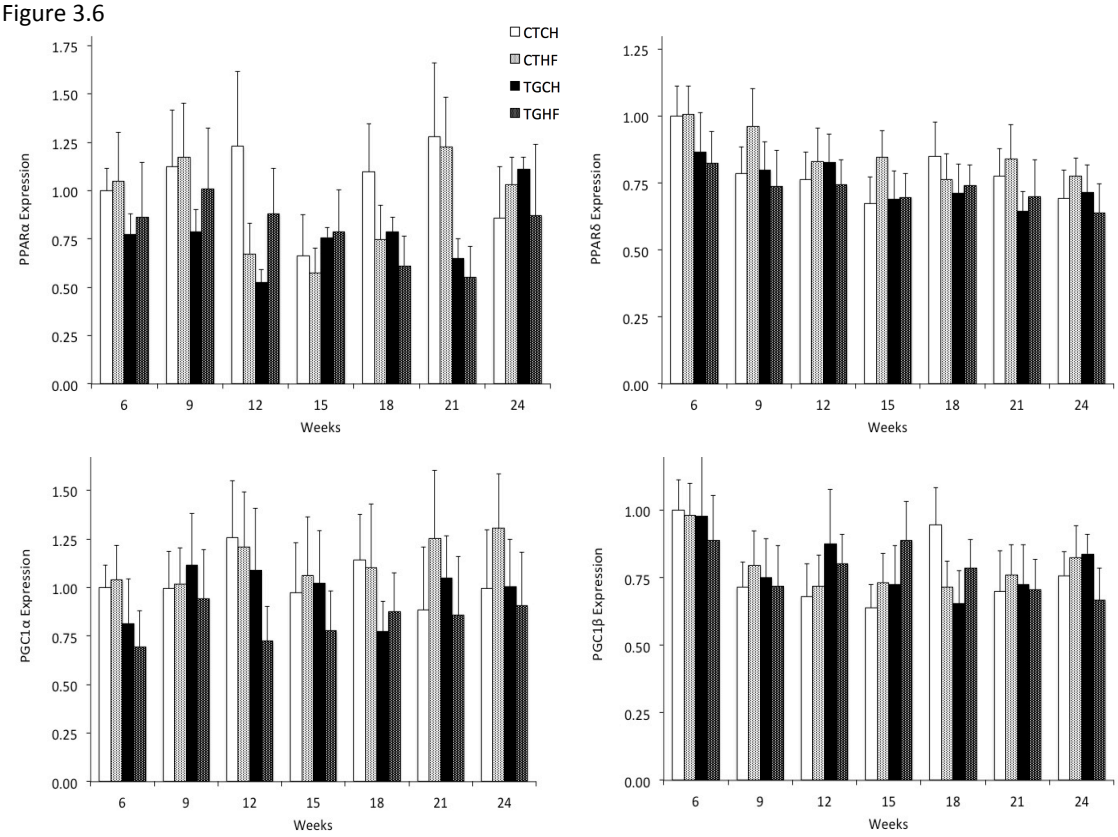
CTCH
CTHF
TGCH
TGHF
PPARα Expression
PPARδ Expression
PGC1α Expression
PGC1β Expression
Weeks
6
9
12
15
18
21
24

Figure 3.7

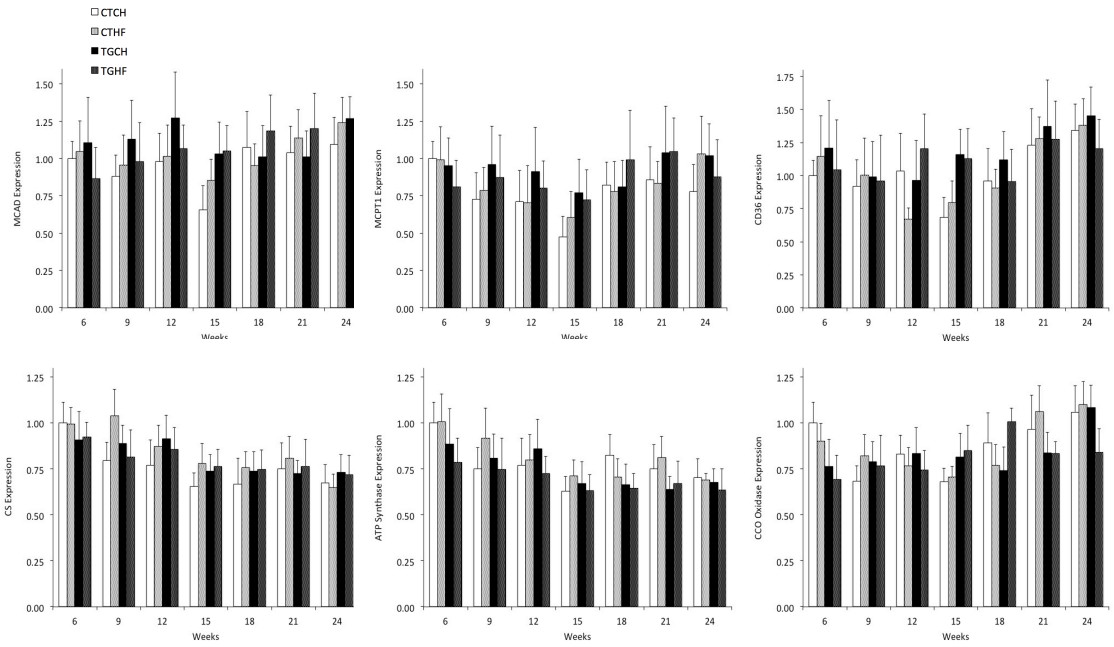
CTCH
CTHF
TGCH
TGHF
MCAD Expression
MCPT1 Expression
CD36 Expression
CS Expression
ATP Synthase Expression
CCO Oxidase Expression
Weeks

CONCLUDING REMARKS

Although there are of multitude of risk factors that influence the development of diabetes, two primary factors are obesity and inactivity. There is a strong correlation between obesity and diabetes, and approximately 80% of type 2 diabetics are obese. Similarly, there is strong correlation between inactivity and diabetes. However, the mechanisms responsible for the development of diabetes under conditions of increasing adiposity and inactivity are unknown. A better understanding of the temporal effects that obesity and inactivity have on the development of diabetes is required. This dissertation investigated the independent effects that obesity and inactivity had on the development of a diabetic phenotype and described the temporal changes in glucose metabolism, mitochondrial function, and body composition.

Due to data demonstrating that increased pancreatic lipids were associated with a reduction in β-cell function, it was proposed that increases in intramuscular triglyceride content could cause mitochondrial dysfunction, which would then lead to the development of diabetes. In this study, prolonged high-fat feeding was associated with significantly greater overall body mass and fat mass. Intramuscular triglyceride content and plasma insulin were also greater in high-fat fed transgenic mice. These factors along with noted decrements in glucose metabolism are hallmarks of developing diabetic phenotype. However, we saw no evidence of mitochondrial dysfunction, as gene expression of key transcriptional regulators was not significantly different among groups. Additionally, there were no differences in the activity levels of two key metabolic enzymes, citrate synthase or cytochrome c oxidase. Therefore, this data does not support the lipotoxicity theory, but instead demonstrates that increased IMTG content, in association with a developing diabetic phenotype, precedes changes in mitochondrial function.

Denervation is often used as a model of inactivity. However, investigations into the effects of denervation-induced inactivity often focus on short-term effects from as soon as 3 hours post-surgery up to 2 weeks after surgery. Atrophic mechanisms are quickly up-regulated following denervation, but the rate of atrophy slows significantly approximately 20-25 days post-surgery. In early time points, we noted decrements in glucose metabolism similar to those reported previously; however, after the rate of

atrophy had slowed there was a compensatory effect of increased glucose uptake. The primary transporter of glucose into skeletal muscle is GLUT4 and the expression of GLUT4 protein mirrored the changes we saw in glucose metabolism, with lower expression in early time points and greater expression in later time points after atrophy has slowed. Protein expression of Akt, a key component of the insulin-signaling pathway, was also greater in later time points. Expression of transcriptional regulators of metabolism, including PPARα, PPARδ, PGC-1α, and PGC-1β, were all lower in denervated tissues throughout the time course of the experiment. Therefore, although metabolic regulation appears to be negatively affected, glucose transport and insulin signaling mechanisms appear to attempt to compensate to improve glucose metabolism.

The exponential increase in the rate of diabetes worldwide is a clarion call for continued research into the pathophysiology of the disease. Although there are a multitude of factors that affect the development of diabetes, this dissertation advances our understanding of the etiology of two key factors, obesity and diabetes.